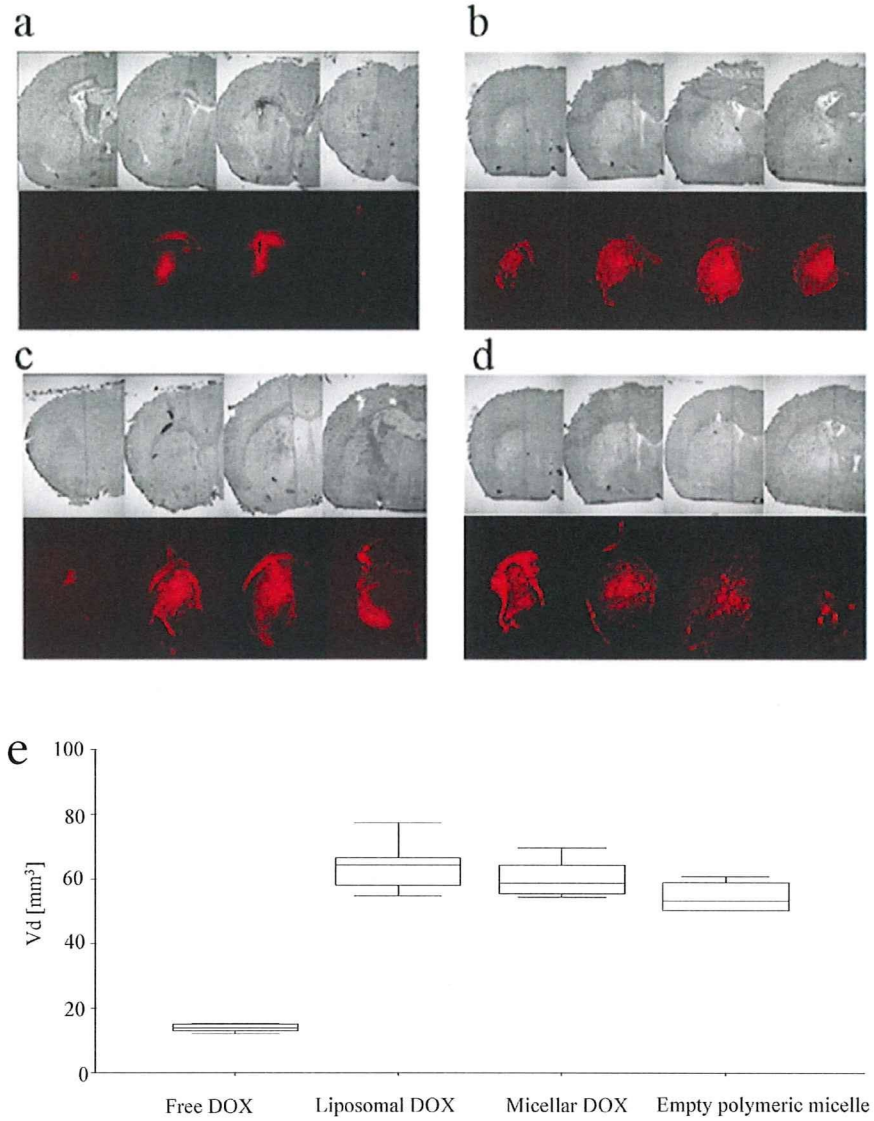

Fig. 1. Evaluation of distribution of micellar DOX in normal rats. Sequential hematoxylin and eosin-stained sections 25 μm thick at 1-mm intervals reveal the tumor (top). The sections were examined with a fluorescence microscope to detect the fluorescence generated by DOX (bottom). Compared with free DOX (a), liposomal DOX (b), micellar DOX (c), and empty polymeric micelles (d) produced extensive and diffuse distribution in the striatum. (e) Median values and the 75% quartiles of volume distribution (Vd) after infusion of free DOX, liposomal DOX, micellar DOX, and empty polymeric micelles. The difference in the distribution between free DOX and micellar DOX was statistically significant ($p = 0.009$, as analyzed by Mann-Whitney *U*-test), but differences in the distribution among liposomal DOX, micellar DOX, and empty polymeric micelles were not.

site but did not develop neurological symptoms. Rats that received 0.1 mg/ml micellar DOX (Fig. 3a, left) showed negligible tissue damage and survived without neurological symptoms. Rats infused with 0.1 (Fig. 3b, left) and 0.4 (Fig. 3b, right) mg/ml free DOX showed tissue damage without neurological symptoms. Rats infused with 0.1 (Fig. 3c, left) and 0.4 (Fig. 3c, right) mg/ml liposomal DOX revealed less tissue damage. Therefore, the maximum tolerated dose of micellar DOX was established as below 0.2 mg/ml. Rats treated with empty polymeric micelles showed no toxicity (data not shown).

Antitumor Efficacy of Micellar DOX Treatment

Rats in the control group (Fig. 4a) were all euthanized at 10–21 days after tumor cell implantation due to neurological symptoms indicative of tumor progression. Median survival for this group was 16.9 days. Rats that received CED of free DOX (Fig. 4b) were euthanized due to neurological complications indicative of tumor progression at 16–33 days after tumor cell implantation. Median survival for this group was 19.6 days. Rats that received CED of 0.2 mg/ml liposomal DOX

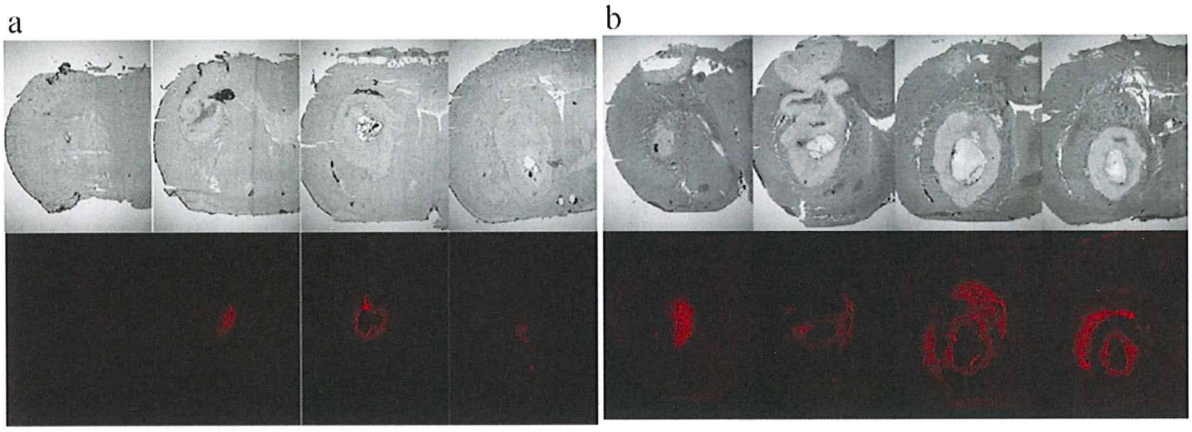

Fig. 2. Evaluation of distribution of micellar DOX in rats with 9L tumors. Seven days after tumor cell implantation, 2 mg/ml free DOX or micellar DOX was infused intratumorally by CED. Rats were euthanized 1 h after CED, and the brains were sectioned on a cryostat. Sequential hematoxylin and eosin-stained sections 25 μm thick at 1-mm intervals reveal the tumor (top). The same sections were examined with a fluorescence microscope to detect the fluorescence generated by DOX (bottom). Free DOX had poor distribution (a), whereas micellar DOX achieved coverage of almost the entire tumor mass, including the surrounding tumor margins (b). The findings were consistent in all four animals.

(Fig. 4c) were euthanized at 10–27 days after tumor cell implantation. Median survival for this group was 16.6 days. Formation of large tumors was verified in all rats euthanized in these three groups. Nine of the 11 rats that received CED of 0.2 mg/ml micellar DOX (Fig. 4d) were euthanized at 15–43 days after tumor cell implantation due to neurological symptoms, but the other two rats survived until termination of the study at 90 days. Median survival for this group was 36 days. The survival time after CED with 0.2 mg/ml micellar DOX was significantly greater than after CED with free DOX (p = 0.0173) or liposomal DOX (p = 0.0007). Although the rats in the control group had histological signs of tumor in the brain (Fig. 4e), only a small amount of brain damage was observed in the surviving two rats that received micellar DOX (Fig. 4f).

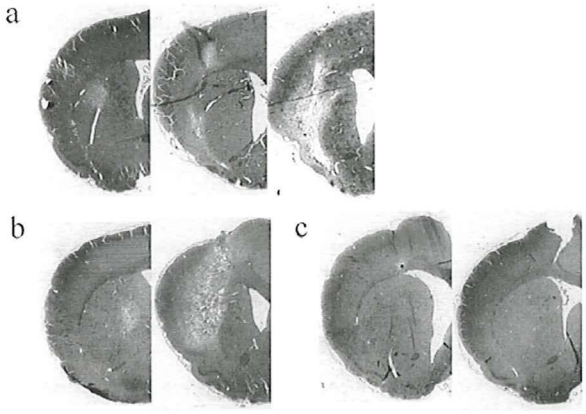

Fig. 3. Toxicity at different drug concentrations. (a) Rats infused with 0.1 mg/ml micellar DOX (left) survived without neurological symptoms and negligible tissue damage. Rats infused with 0.2 (center) and 0.4 (right) mg/ml micellar DOX showed significant tissue damage at the infusion site but did not develop neurological symptoms. (b) Rats infused with 0.1 (left) and 0.4 (right) mg/ml free DOX demonstrated tissue damage without neurological symptoms. (c) Rats infused with 0.1 (left) and 0.4 (right) mg/ml liposomal DOX revealed less tissue damage, which might reflect the poor drug release.

Discussion

The present study found that liposomal DOX and micellar DOX had similar extensive distributions in the normal rat brain and were far more widely distributed than free DOX. This study also showed distribution of micellar DOX over almost the entire tumor area, including the margins. CED distribution in CNS is significantly increased if the infusate is more hydrophilic, which implies less tissue affinity.[9,11] Furthermore, polyethylene glycol encapsulation provides steric stabilization, reduces surface charge, and achieves better distribution in brain.[9] The poorer brain distribution observed with hydrophobic or cationic infusate can be completely overcome by polyethylene glycol encapsulation.[9]

Delivery pattern of micellar DOX was expected to avoid the high peak concentrations of free DOX potentially associated with toxicity.[13,25] However, evaluation of the toxicity in normal rat brain found that 0.2 mg/ml micellar DOX caused a lesion similar to that caused by 0.2 mg/ml free DOX, although no difference in toxicity was observed. In contrast, 0.2 mg/ml liposomal DOX showed no toxicity, which might reflect poor release of the cytotoxic agent. These findings indicate that the safety of micellar DOX in CED could be achieved by optimization of drug release to avoid the high concentrations that trigger nonspecific toxicity. Micellar systems, relative to liposomal systems, offer the advantage of adjustable drug release based on the properties of the

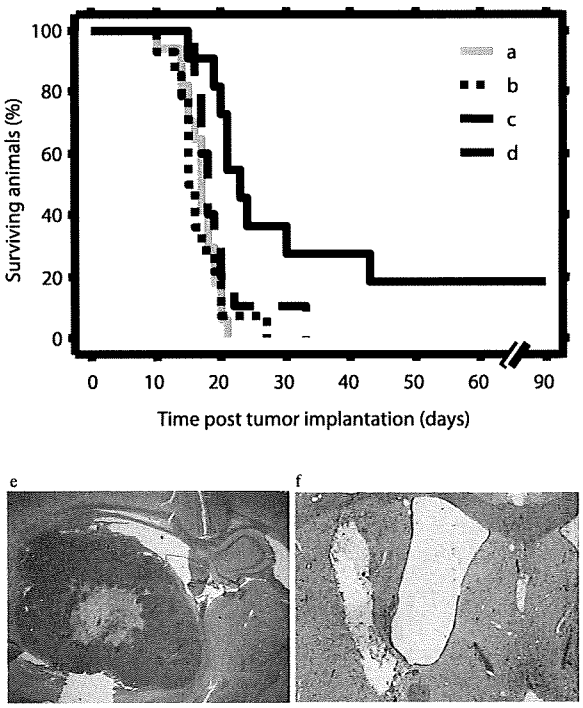

Fig. 4. Survival study. (a–d) Outcome for rats bearing 9L tumors with single CED infusion of saline (a), free DOX (b), liposomal DOX (c), and micellar DOX (d). Seven days after tumor implantation within the brain, rats were treated with 0.2 mg/ml of each agent. Median survival for the groups were 16.9 days (a), 19.6 days (b), 16.6 days (c), and 36 days (d). Statistically significant differences were observed between free DOX and micellar DOX ($p = 0.0173$) and between liposomal DOX and micellar DOX ($p = 0.0007$). (e and f) Histological examination found tumor formation in the control group (e) and brain damage in rats receiving micellar DOX (f).

micelle inner core,[13–16,25] but further development of micellar systems for use with CED is required.

The present study found that CED with 0.2 mg/ml micellar DOX significantly prolonged survival in rats with intracranial 9L glioma, compared with CED with 0.2 mg/ml free DOX and liposomal DOX, which is known to show efficient targeting to solid tumors by systemic injection like micellar DOX. Liposomal DOX does not release DOX efficiently because of excessive stable incorporation in the lipid bilayer,[17] which probably accounts for the absence of significant increase in efficacy against rapidly growing 9L syngeneics compared with free DOX.

The polymeric micelle system has three advantages as a drug carrier compared with the liposome drug carrier. First, polymeric micelles can incorporate hydrophobic drugs into the inner core phase, to high loadings such as 30 wt% without losing targeting potential. In contrast, the liposomal system may easily lose targeting ability at high drug loadings because the hydrophobic drug must be incorporated into the very thin lipid bilayer. Second, polymers may be based on many chemical structures with various physical characteristics such as crystalline and glassy, so the drug release rate can be adjusted in a very wide range from minutes to days. Finally, micelle diameters can be tightly controlled in a range from 10 nm to 100 nm, choosing the appropriate chemical structures and chain lengths of polymers. The polymeric micelle can obtain this size control among many types of drug carriers. Consequently, the micelle system has high potential for specific adjustment to the treatment of various CNS tumors by CED infusion. Furthermore, micellar systems could be used in monitoring drug distribution by using micelles containing a marker for imaging.[23,24] The present findings indicate the significant potential of micellar drugs for the treatment of malignant glioma.

References

1. Bobo RH, Laske DW, Akbasak A, Morrison PF, Dedrick RL, Oldfield EH. Convection-enhanced delivery of macromolecules in the brain. *Proc Natl Acad Sci USA.* 1994;91:2076–2080.
2. Bruce JN, Falavigna A, Johnson JP, et al. Intracerebral clysis in a rat glioma model. *Neurosurgery.* 2000;46:683–691.
3. Degen JW, Walbridge S, Vortmeyer AO, Oldfield EH, Lonser RR. Safety and efficacy of convection-enhanced delivery of gemcitabine or carboplatin in a malignant glioma model in rats. *J Neurosurg.* 2003;99:893–898.
4. Kaiser MG, Parsa AT, Fine RL, Hall JS, Chakrabarti I, Bruce JN. Tissue distribution and antitumor activity of topotecan delivered by intracerebral clysis in a rat glioma model. *Neurosurgery.* 2000;47:1391–1399.
5. Vogelbaum MA. Convection enhanced delivery for treating brain tumors and selected neurological disorders: symposium review. *J Neurooncol.* 2007;83:97–109.
6. Kunwar S, Prados MD, Chang SM, et al. Cintredekin Besudotox Intraparenchymal Study Group. Direct intracerebral delivery of cintredekin besudotox (IL13-PE38QQR) in recurrent malignant glioma: a report by the Cintredekin Besudotox Intraparenchymal Study Group. *J Clin Oncol.* 2007;25:837–844.
7. Wu G, Yang W, Barth RF, et al. Molecular targeting and treatment of an epidermal growth factor receptor-positive glioma using boronated cetuximab. *Clin Cancer Res.* 2007;13:1260–1268.
8. Krauze MT, Noble CO, Kawaguchi T, et al. Convection-enhanced delivery of nanoliposomal CPT-11 (irinotecan) and PEGylated liposomal doxorubicin (Doxil) in rodent intracranial brain tumor xenografts. *Neuro-Oncology.* 2007;9:393–403.
9. Yamashita Y, Krauze MT, Kawaguchi T, et al. Convection-enhanced delivery of a topoisomerase I inhibitor (nanoliposomal topotecan) and a topoisomerase II inhibitor (pegylated liposomal doxorubicin) in intracranial brain tumor xenografts. *Neuro-Oncology.* 2007;9:20–28.

10. Noble CO, Krauze MT, Drummond DC, et al. Novel nanoliposomal CPT-11 infused by convection-enhanced delivery in intracranial tumors: pharmacology and efficacy. *Cancer Res.* 2006;66:2801–2806.
11. Saito R, Bringas JR, McKnight TR, et al. Distribution of liposomes into brain and rat brain tumor models by convection-enhanced delivery monitored with magnetic resonance imaging. *Cancer Res.* 2004;64:2572–2579.
12. MacKay JA, Deen DF, Szoka FC Jr. Distribution in brain of liposomes after convection enhanced delivery; modulation by particle charge, particle diameter, and presence of steric coating. *Brain Res.* 2005;1035:139–153.
13. Yokoyama M, Miyauchi M, Yamada N, et al. Characterization and anticancer activity of the micelle-forming polymeric anticancer drug Adriamycin-conjugated poly(ethylene glycol)-poly(aspartic acid) block copolymer. *Cancer Res.* 1990;50:1693–1700.
14. Yokoyama M, Fukushima S, Uehara R, et al. Characterization of physical entrapment and chemical conjugation of Adriamycin in polymeric micelles and their design for in vivo delivery to a solid tumor. *J Control Release.* 1998;50:79–92.
15. Fukushima S, Machida M, Akutsu T, et al. Role of Adriamycin and Adriamycin dimer in antitumor activity of the polymeric micelle carrier system. *Colloids Surf B Biointerfaces.* 1999;16:227–236.
16. Yokoyama M, Okano T, Sakurai Y, et al. Selective delivery of Adriamycin to a solid tumor using a polymeric micelle carrier system. *J Drug Target.* 1999;7:171–186.
17. Tsukioka Y, Matsumura Y, Hamaguchi T, et al. Pharmaceutical and biomedical differences between micellar doxorubicin (NK911) and liposomal doxorubicin (Doxil). *Jpn J Cancer Res.* 2002;93:1145–1153.
18. Greish K. Enhanced permeability and retention of macromolecular drugs in solid tumors: a royal gate for targeted anticancer nanomedicines. *J Drug Target.* 2007;15:457–464.
19. Hamaguchi T, Kato K, Yasui H, et al. A phase I and pharmacokinetic study of NK105, a paclitaxel-incorporating micellar nanoparticle formulation. *Br J Cancer.* 2007;97:170–176.
20. Uchino H, Matsumura Y, Negishi T, et al. Cisplatin-incorporating polymeric micelles (NC-6004) can reduce nephrotoxicity and neurotoxicity of cisplatin in rats. *Br J Cancer.* 2005;93:678–687.
21. Kawano K, Watanabe M, Yamamoto T, et al. Enhanced antitumor effect of camptothecin loaded in long-circulating polymeric micelles. *J Control Release.* 2006;112:329–332.
22. Koizumi F, Kitagawa M, Negishi T, et al. Novel SN-38-incorporating polymeric micelles, NK012, eradicate vascular endothelial growth factor-secreting bulky tumors. *Cancer Res.* 2006;66:10048–10056.
23. Amirbekian V, Lipinski MJ, Briley-Saebo KC, et al. Detecting and assessing macrophages in vivo to evaluate atherosclerosis noninvasively using molecular MRI. *Proc Natl Acad Sci USA.* 2007;104:961–966.
24. Lepage M, Jiang J, Babin J, Qi B, Tremblay L, Zhao Y. MRI observation of the light-induced release of a contrast agent from photo-controllable polymer micelles. *Phys Med Biol.* 2007;52:249–255.
25. Yokoyama M, Okano T, Sakurai Y, Ekimoto H, Shibazaki C, Kataoka K. Toxicity and antitumor activity against solid tumors of micelle-forming polymeric anticancer drug and its extremely long circulation in blood. *Cancer Res.* 1991;51:3229–3236.

Journal of Controlled Release xxx (2009) xxx–xxx

Contents lists available at ScienceDirect

Journal of Controlled Release

journal homepage: www.elsevier.com/locate/jconrel

Preparation and in vivo imaging of PEG-poly(L-lysine)-based polymeric micelle MRI contrast agents

Kouichi Shiraishi [a], Kumi Kawano [b], Takuya Minowa [b], Yoshie Maitani [b], Masayuki Yokoyama [a,*]

[a] Kanagawa Academy of Science and Technology, Yokoyama "Nano-medical Polymers" Project, KSP East 404, Sakado 3-2-1, Takatsu-ku, Kawasaki, Kanagawa 213-0012, Japan
[b] Institute of Medicinal Chemistry, Hoshi University, 2-4-41 Ebara, Shinagawa-ku, Tokyo 142-8501, Japan

ARTICLE INFO

Article history:
Received 24 October 2008
Accepted 17 January 2009
Available online xxxx

Keywords:
Polymeric micelle
MRI contrast agent
Long circulation
Tumor imaging
Poly(ethylene glycol)-b-poly(L-lysine)

ABSTRACT

A polymeric micelle drug carrier system was applied to the targeting of an MRI (magnetic resonance imaging) contrast agent. A block copolymer, PEG-*b*-poly(L-lysine), was used for conjugation of gadolinium ions through chelating moieties, DOTA. The DOTA moieties were successfully conjugated to all primary amine groups of the lysine residues. The obtained block copolymer, PEG-*b*-poly(L-lysine-DOTA), formed a polymeric micelle. The polymeric micelle structure was maintained even after partial gadolinium chelation (~40%) to the DOTA moieties. The prepared polymeric micelle MRI contrast agent was injected into a mouse tail vein at a dose of 0.05 mmol Gd/kg. The polymeric micelle-based MRI contrast agent exhibited stable blood circulation. A considerable amount (6.1 ±0.3% of ID/g of the polymeric micelle) was found to accumulate at solid tumors 24 h after intravenous injection by means of the EPR effect. An MRI analysis revealed that the signal intensity of the tumor was enhanced 2.0-fold by the use of this contrast agent.

1. Introduction

Various types of nano-sized drug carriers including linear synthetic polymers, dendrimers, proteins, liposomes, and polymeric micelles have been investigated for anti-cancer drug targeting to solid tumor sites for improvements in cancer chemotherapy [1,2]. Among these nano-sized carrier systems, polymeric micelles have been studied with a focus on encapsulation of hydrophobic drugs [3]. Most typically, polymeric micelles are constituted of block copolymers having a hydrophilic chain such as PEG and a hydrophobic chain. The hydrophobic chain can form a hydrophobic inner core that incorporates hydrophobic drugs. A strong advantage of the polymeric micelles is their high structural stability in the bloodstream and their very small size, being in a range of 10–100 nm. This size range is preferable for the passive targeting of solid tumors by means of the EPR (enhanced permeability and retention) effect [3]. Successful tumor-targeting-carrier systems include the adriamycin-incorporated polymeric micelle system [1], which involves a metal complex drug-incorporated (e.g., cisplatin-incorporated) polymeric system [4–6].

The recent study reported that several nano-sized-carrier system and, in particular, diagnostic imaging agents rest on drug-targeting methodology. Magnetic resonance imaging (MRI) is a non-invasive imaging modality for diagnosis. Owing to rapid developments in temporal and spatial resolution, the value of MRI has grown greater in recent decades. Nowadays, much attention is given to MRI contrast agents both of low molecular weight and of macromolecule status for their ability to improve MRI signals.

Paramagnetic metal complexes, such as the gadolinium (III) ion–DTPA complex, are widely used in clinical diagnosis. Such gadolinium complexes enhance T_1-weighted images by shortening the T_1-relaxation time of the water protons. Linear polymers such as dextran [7,8], poly(L-lysine) [9,10], poly(glutamic acid) [11–13], and poly[N-(2-hydroxypropyl)methacrylamide] [14] have been investigated as possible for carriers of the gadolinium complexes. Dendrimers, which possess well-defined structures and accurate molecular weights, have also attracted much attention as carriers of MRI contrast agents because dendrimers' biodistribution were depend on the generations [15–17].

Polymeric micelle-based MRI contrast agents also have a potential as MRI contrast agents. Because the polymeric micelle is an associate of many block copolymer chains, block copolymers with well-controlled molecular weight can be excreted through kidney filtration after dissociation of the polymeric micelles into block copolymer chains. Therefore, a low risk of chronic toxicity is expected to present itself and is expected to stem from polymeric micelles' complete excretion over a long time period. On the other hand, polymeric micelles can exhibit a preferential pharmacokinetic profile in a defined time period required for the targeting of tumors. In a previous report, we prepared a polyion complex micelle from charged block copolymers and counter ionic polymers [18]. This polymeric micelle MRI contrast agent possessed the characteristic of changeable T_1-relaxivity: The polymeric micelle exhibited a lower T_1-relaxivity than did block copolymer chains having dissociated from the micelle. This changeable character can be utilized as a tumor-specific MRI contrast

* Corresponding author. Tel.: +81 44 819 2093; fax: +81 44 819 2095.
E-mail address: yp-yokoyama2093ryo@newkast.or.jp (M. Yokoyama).

0168-3659/$ – see front matter © 2009 Elsevier B.V. All rights reserved.
doi:10.1016/j.jconrel.2009.01.010

Please cite this article as: K. Shiraishi, et al., Preparation and in vivo imaging of PEG-poly(L-lysine)-based polymeric micelle MRI contrast agents, J. Control. Release (2009), doi:10.1016/j.jconrel.2009.01.010

with a high MRI contrast (in dissociate form) at tumor tissues and a low MRI contrast (in micelle form) in the bloodstream. In the previous report, we proved this changeable character in vitro, but did not examine in vivo tumor targeting.

Several works on polymeric micelles as MRI contrast agents were reported recently [19–22]. The combination of drug targeting and imaging probes, such as MRI contrast agents, relative to polymer micelles systems has strengthened the effectiveness of chemotherapy [23]. Poly(L-glutamic acid)-*b*-polylactide and polysucciucinimicde derivatives were synthesized as a polymeric micelle-based MRI contrast agent [20,21]. Several studies have examined polymeric micelle-based MRI contrast agents, but so far, significant enhancements of MR images at solid tumors through accumulation of the polymeric micelles have not been obtained. One of the challenges that confront the use of MRI contrast agents to detect solid tumors is the selective delivery of the contrast agents to solid tumors by means of the EPR effect. From our experience of anti-cancer drug targeting with polymeric micelle carriers, we assume that an important key for successful tumor targeting is suppression of the incorporated drug's interactions with cells and proteins, in particular, hydrophobic interactions. In our previous report, we showed that polymeric micelles exhibiting lower levels of hydrophobic interactions provided higher levels of antitumor activities, possibly through more efficient passive targeting [24]. If this assumption is applied to MRI contrast agents, the micelle outer shell with a biologically inert character is preferable. Therefore, we have chosen a micelle design with the inert poly(ethylene glycol) outer shell and the contrast species (Gd ion)-containing inner core. Furthermore, we have chosen a negatively charged inner core, not a positively charged one, since positive charges are known to induce strong interactions with the reticuloendothelial system (RES) [25]. Consequently, strong interactions with the RES drastically lower the targeting efficiency relative to solid tumors.

In this report, we synthesized negatively charged block copolymers based on a poly(ethylene glycol)-*b*-poly(L-lysine) system to obtain a long-circulating polymeric micelle MRI contrast agent. This negatively charged block copolymer was found to form a polymeric micelle structure without an addition of positively charged macromolecules. Blood circulation, biodistribution, and excretion of the contrast agents were evaluated. MR images of mice were taken after an injection of the contrast agent, and these images were compared before the injection. According to the findings, polymeric-micelle MRI contrast agent appears to be a strong tool for polymeric-micelle-based drug targeting and for visualizing the location of the carriers at the solid tumor tissues.

2. Materials and methods

2.1. Materials

For the current study, α-methoxy-ω-aminopropyl-poly(ethylene glycol) (PEG-NH_2, M_w=5200) was purchased from NOF Corporation, Tokyo, Japan, and benzene-based lyophilization was carried out before use. A chelating agent active ester, 1,4,7,10-tetraazacyclododecane-1,4,7,10-tetraacetic acid mono (*N*-hydroxysuccinimide ester) (DOTA-OSu), was purchased from Macrocyclics, Texas, USA. Deuterium solvents were purchased from Sigma-Aldrich, Tokyo, Japan. Dehydrated DMF and gadolinium chloride hexahydrate ($GdCl_3 \cdot 6H_2O$) were purchased from Wako Pure Chemicals Industries, Ltd., Tokyo, Japan. We used all these commercial reagents as purchased. The dialysis membrane Spectrapor 6 (molecular weight cut off (MWCO)= 1000) was purchased from Spectrum Laboratories Inc., Tokyo, Japan. ^{1}H NMR spectra were recorded on a Varian UNITY INOVA 400 MHz NMR spectrometer. To measure gadolinium ion contents in the block copolymer, we used inductively coupled plasma (ICP) with an SPS7800 apparatus (SII NanoTechnology Inc., Tokyo, Japan). Dynamic

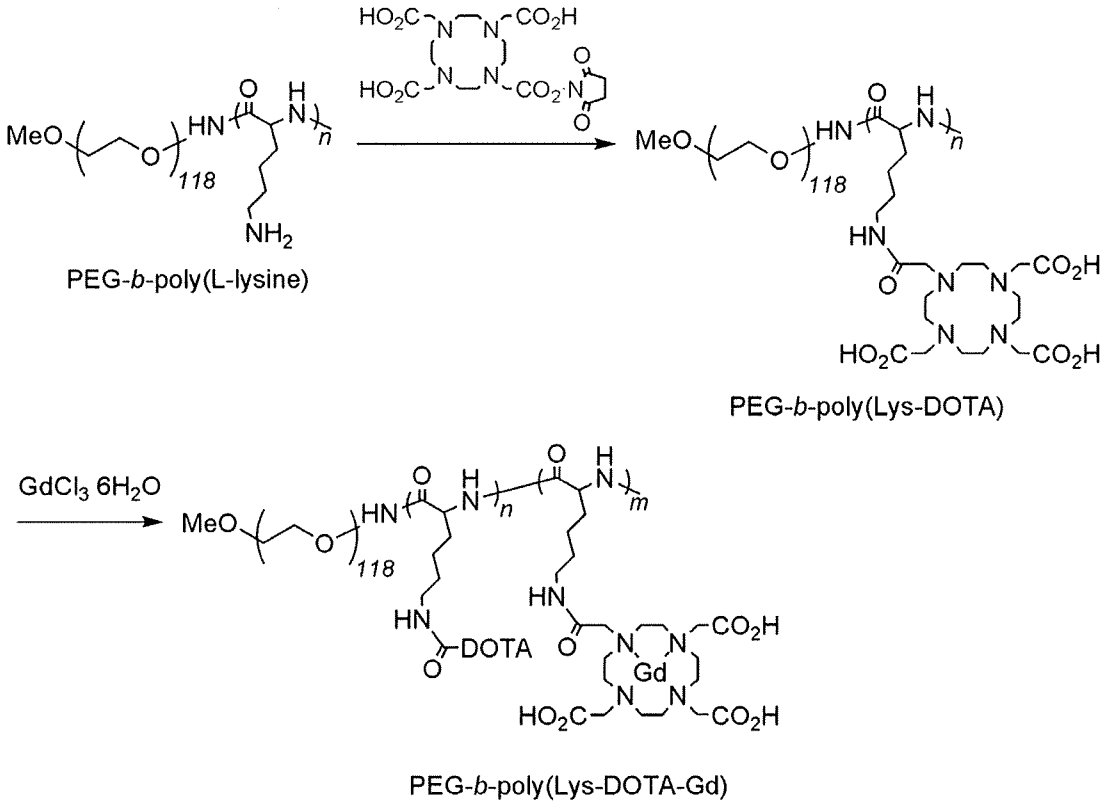

Fig. 1. Synthesis of PEG-P(Lys-DOTA-Gd).

Please cite this article as: K. Shiraishi, et al., Preparation and in vivo imaging of PEG-poly(L-lysine)-based polymeric micelle MRI contrast agents, J. Control. Release (2009), doi:10.1016/j.jconrel.2009.01.010

light scattering (DLS) measurements were carried out at 24.5 °C with a DLS-700 instrument (Otsuka Electronics Co., Ltd., Tokyo Japan). Measurement of zeta-potential was performed with an ELSZ-2 instrument (Otsuka Electronics Co., Ltd., Tokyo Japan).

2.2. Animals

Five-week-old ddY female mice and CDF_1 female mice were purchased from the Sankyo Labo Service Corporation, Tokyo, Japan. All animal experiments were carried out in accordance with the guidelines of the Guiding Principles for the Care and Use of laboratory Animals of Hoshi University.

2.3. Synthesis of PEG-P(Lys-DOTA)

A synthesis of a chelate moiety-binding block copolymer is shown in Fig. 1. A poly(ethylene glycol)-*b*-poly(L-lysine) block copolymer (PEG-P(Lys)) was prepared through acid hydrolysis of a poly(ethylene glycol)-*b*-poly[ε-(benzyloxycarbonyl)-L-lysine] (PEG-P(Lys(Z)) block copolymer [26]. We synthesized PEG-P(Lys)s from PEG-NH_2 (molecular weight of PEG-NH_2 = 5200). The compositions of PEG-P(Lys)s were determined by means of ^1H NMR in D_2O under an acidic condition. A mixture of PEG-P(Lys) (86.0 mg), and 1,4,7,10-tetraazacyclododecane-1,4,7,10-tetraacetic acid mono (*N*-hydroxysuccinimide ester) (DOTA-OSu, 308.0 mg) in 8.6 mL of dry DMF was stirred, and then, dry triethylamine (0.5 mL) was added to this reaction mixture. The reaction mixture was stirred overnight at 50 °C. The resulting mixture was dialyzed, at first, against 0.02 N HCl and, then, against distilled H_2O 5 times. The obtained polymer was dissolved in H_2O (at a polymer concentration higher than 15 mg/mL) again, and dialyzed against H_2O 3 times, and we obtained poly(ethylene glycol)-*b*-poly(L-lysine-DOTA) (PEG-P(Lys-DOTA)) by means of lyophilization (162.8 mg). The composition of PEG-P(Lys-DOTA) was determined by means of ^1H NMR in D_2O under an alkali condition (pH > 10). The number of bound DOTA units per polymer chain was calculated from the peak area ratio among CH_2 protons of PEG at 3.73 ppm, 24H protons of DOTA, and 2H protons of lysine in the range of 3.36–2.18 ppm. ^1H NMR (ppm, D_2O + NaOD): 4.08 (s, CH of lysine units), 3.73 (s, CH_2 of PEG), 3.39 (s, OCH_3 of terminal PEG), 3.36–2.18 (m, 24H of DOTA and CH_2 of lysine), and 2.18–1.10 (m, 6H of lysine).

2.4. Gadolinium (III) chelation to PEG-P(Lys-DOTA)

$GdCl_3 \cdot 6H_2O$ (35.0 mg, 0.094 mmol) was added to PEG-P(Lys-DOTA) (153.3 mg) in H_2O (15.0 mL), and the pH of the solution was maintained between 6.0–6.5. The reaction mixture was stirred for 3 h at 50 °C, followed by dialysis against distilled H_2O 5 times. PEG-P(Lys-DOTA-Gd) was obtained as a white solid after lyophilization (160.8 mg). The determination of gadolinium ions in the block copolymer was carried out by means of ICP measurements (7.0 wt.%, the number of gadolinium ions per polymer chain was 6.7). The obtained PEG-P(Lys-DOTA-Gd) is indicated as 118-17-17-7 (PEG unit = 118, lysine units = 17, DOTA moieties = 17, number of gadolinium ion = 7).

2.5. Blood concentration of PEG-P(Lys-DOTA-Gd) micelles in mice

Blood samples (10–75 μL) from the tail vein (n = 3) of mice (ddY) (30–33 g) were collected in heparinized capillary glass. Saline (1.5 mL) was added to the blood samples, and the mixture was centrifuged at 4 °C for 4 min at 13,000 rpm. The supernatant of the plasma solution was collected, and the gadolinium ion contents of the block copolymer were measured by means of ICP. The plasma and blood volume were calculated as 0.0488 mL/g body weight for plasma and 0.0778 mL/g body weight for blood, respectively.

2.6. Biodistribution of the contrast agents

Biodistribution of the contrast agents was evaluated in CDF_1 female mice (5 weeks old) (20–22 g) bearing a colon 26 tumor. Colon 26 cells (1.0×10^4 cells/0.1 mL) were transplanted into CDF_1 female mice subcutaneously. Injection of the contrast agents was started 9–10 days after the transplantation. Tumor volumes were approximately 50–100 mm^3. The tumor volumes were calculated as follows: volume = $1/2LW^2$; L is the long diameter and W is the short diameter of a tumor.

Twenty-four hours after the injection, the blood was collected with a heparinized syringe and centrifuged at 4 °C for 4 min at 13,000 rpm. The plasma was obtained, and its gadolinium content was measured by means of ICP. The major tissues including tumor tissues were excised and weighted. For the determination of gadolinium ion content in the tissue, saline was added to the tissues, followed by an addition of nitric acid (conc. 70%) and sulfuric acid (conc. 98%). Then, the mixture was heated. A saturated aqueous oxoammonium solution was added to the yellow mixture and heated again. The resulting pale-yellow mixture was diluted with saline. The supernatant was collected, and its gadolinium content was measured by means of ICP. The urine (n = 3) was collected 24 h and 48 h after injection, and its gadolinium content was measured by means of ICP.

2.7. MR imaging of mice tumor model

MR imaging was performed with female mice (CDF_1) bearing a colon 26 tumor. The tumor transplantation was carried out as described in 2.6. The contrast agents were injected at a dose of 0.05 mmol of Gd/kg into a mice-tail vein. MR images were taken with a Varian NMR system at 9.4 T. T_2-weighted fast spin echo (TR = 2500 ms, ETL = 8, ESP = 4, effective TE = 48) was performed for all experiments before following the T_1-weighted gradient echo protocol. T_1-weighted gradient echo protocol was followed before the injection, immediately after the injection, and then 4 h and 24 h after the injection. Imaging parameters of the T_1-weighted images were TR/TE = 8.0/4.2, flip angle = 30°, field of view of 50 × 30 mm, a matrix size of 192 × 192, and 2 mm of coronal slice thickness, and were TR/TE = 8.0/4.5, flip angle = 30°, field of view of 45 × 45 mm, a matrix size of 192 × 192, and 2 mm of axial slice thickness. For normalized signal intensity relative to the T_1-weighted images, the tumor area was selected as a region of interest (ROI). The signal intensity of the ROI was compared with the intensity of a stock solution of 0.1 mM gadolinium ion in agarose gel.

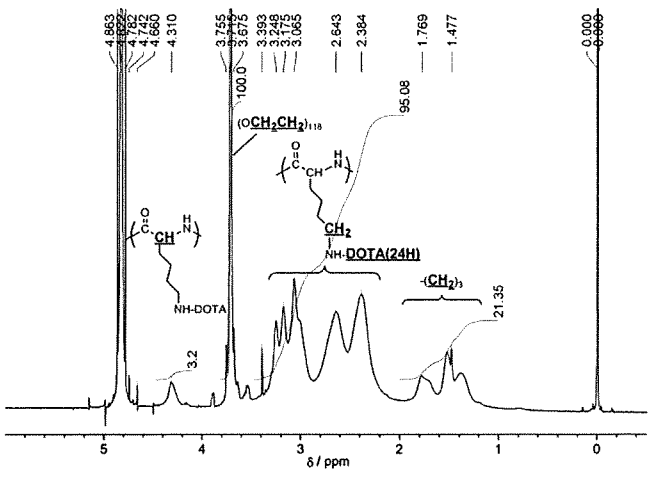

Fig. 2. ^1H NMR spectrum of PEG-P(Lys-DOTA) (118-17-17) in D_2O + NaOD.

Please cite this article as: K. Shiraishi, et al., Preparation and in vivo imaging of PEG-poly(L-lysine)-based polymeric micelle MRI contrast agents, J. Control. Release (2009), doi:10.1016/j.jconrel.2009.01.010

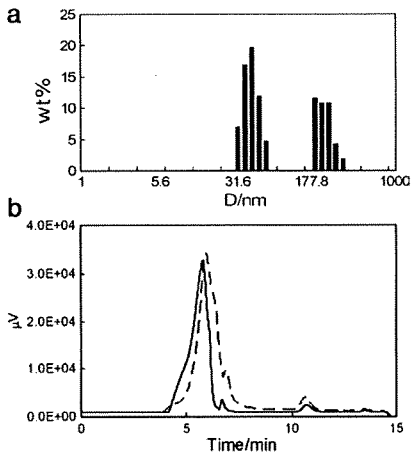

Fig. 3. (a) Weight-weight average size distribution of PEG-P(Lys-DOTA-Gd) micelle (118-17-17-7) in 150 mM NaCl measured by DLS, and (b) gel-permeation chromatogram of PEG-P(Lys-DOTA-Gd) micelle in H_2O (1.2 mg/mL) of concentrated preparation of 118-17-17-7(solid line) and diluted preparation of 118-17-17-6 (dashed line).

The relative signal intensity of the ROI 24 h after the injection was compared with the signal intensity before the injection.

3. Results and discussion

3.1. Block copolymer synthesis and characterization of polymeric micelle

A block copolymer binding DOTA groups was synthesized from poly(ethylene glycol)-*b*-poly(L-lysine). The binding of a DOTA at the lysine residues was carried out with a coupling reaction between a primary amine and an NHS ester of a DOTA reagent, as shown in Fig. 1. Poly(ethylene glycol)-*b*-poly(L-lysine-DOTA) block copolymers possessing 5200 of molecular weights, and 17–21 units of the DOTA-bound lysine moiety were obtained. Quantitative substitution of lysine residues for DOTA was confirmed in ^1H NMR spectra as shown in Fig. 2.

A fully DOTA-substituted block copolymer formed polymeric micelles after the dialysis in dist. H_2O at a polymer concentration of 15 mg/mL. The quantitative DOTA conjugation was essential for the polymeric micelle formation. Insufficient DOTA conjugation, such as 118-22-19 wherein the number of DOTA residues was 19 out of 22 lysine residues, did not form a polymeric micelle. This result shows that the micelle structures were not formed in the presence of a small amount of unmodified lysine residue (3 out of 22 residues); the result also underscores the importance of strong interactions among the conjugation DOTA units for the micelle formation.

Gadolinium ion was partially chelated to DOTA in the block copolymer, poly(ethylene glycol)-*b*-poly(L-lysine-DOTA). Gadolinium-chelated poly(ethylene glycol)-*b*-poly(L-lysine-DOTA-Gd) maintained the polymeric micelle formation. Dynamic light scattering (DLS) and GPC measurements of the gadolinium chelated block copolymers, 118-17-17-7 which is 118 ethylene glycol units, 17 lysine residues, 17 DOTA conjugation to lysine residues, and 7 gadolinium ions at DOTA were performed. Fig. 3(a) shows a DLS chart of this block copolymer micelle with a weight average of 42.9±7.6 nm (mean±SD), accompanied by a secondary aggregation of a weight average of 225.5±53.0 nm (mean±SD). Similar secondary aggregation was also found in the precursor of PEG-*b*-poly(L-lysine-DOTA-Gd) (data in supplemental section).

The zeta-potential of the obtained polymeric micelle showed −9.55 mV in 150 mM NaCl solution, indicating that the polymeric micelle was negatively charged. This negative value was given from a vacant DOTA moiety having 3 carboxylic acids and 4 tertiary amines. The tertiary amines of DOTA could work as only two cationic species in the physiological condition owing to their excessively close proximity to each other, whereas three carboxylic acids in the DOTA moiety could work as 3 anions owing to their long distances from one other. As a result, the total charge of the polymeric micelles exhibited negatively charged particles. In general, cationic species are more quickly scavenged by the reticloendothelial system than anionic species [25]. This scavenging is a big obstacle for the passive tumor targeting through the EPR effect. For the design of a tumor-targeting system, a slightly negative-charged particle is preferable as an inert carrier.

GPC measurements of the polymeric micelle (1.2 mg/mL in H_2O) were performed by the use of an HPLC system (LC 2000 series, Jasco, Tokyo, Japan) equipped with a TSK-gel G4000-PW_{XL} column (eluent=H_2O, flow rate=1.0 mg/mL, detector=RI) at 40 °C. Even in such a diluted aqueous solution of the block copolymer, both DLS and GPC measurements clearly exhibit the formation of the polymeric micelle as shown in Fig. 3(b) (solid line). This finding indicated that once the polymeric micelle was formed by interactions among vacant DOTAs, the polymeric micelle was not dissociated in a time scale of a DLS and GPC measurement under dilution. When we injected a similar sample 118-17-17-6 prepared from a dilute condition (3 mg/mL), the peak of the polymeric micelle was shifted to a longer elution time as shown in Fig. 3(b) (dashed line). This result indicates a considerable polymer concentration effect on the formation of the polymeric micelle; namely, strong interactions among vacant DOTA moieties at a high concentration.

Formation of the polymeric micelle with or without a gadolinium ion appears to depend on interactions among vacant DOTAs as described above. To prove this interaction, we added an excess of $GdCl_3$ (2.0 mol equivalent vs DOTA) into 118-20-20 to prepare complete chelation of the DOTA units with gadolinium ions. However, we found that the composition of the block copolymer was 118-20-20-16. Even when we added the excess amount of gadolinium ions to the block copolymer, we obtained 20% of vacant DOTA in the block copolymer. This result implies that DOTA–DOTA interactions prevent gadolinium ion from freely chelating into a DOTA moiety. When we injected this block copolymer into the GPC column, we observed that the peak of around 5–6 min. corresponded to the polymeric micelle disappeared. This disappearance indicates that chelation of a high level of gadolinium ion in a block copolymer resulted in so unstable micelle formation on the GPC column. We concluded that the polymeric micelle was formed through the interactions among vacant DOTAs, and that these interactions depend on the block copolymer concentrations and on the numbers of the chelated gadolinium ions.

3.2. Blood circulation of the polymeric micelle MRI contrast agent

The polymeric micelle, 118-17-17-7, was injected at a dose of 0.05 mmol Gd/kg, into a mouse-tail vein for pharmacokinetic

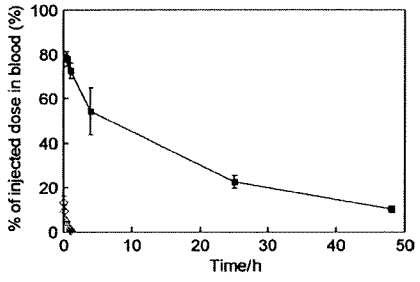

Fig. 4. Blood-concentration time course of PEG-P(Lys-DOTA-Gd) micelle (118-17-17-7) in ddY female mice at a dose of 0.05 mmol Gd/kg (■), and Gd-DTPA at a dose of 0.10 mmol Gd/kg (◇). After defined time periods (0.5 h, 1 h, 2 h, 4 h, 24 h, and 48 h), the blood samples were collected into capillary glass tubes via mice's tail veins.

Please cite this article as: K. Shiraishi, et al., Preparation and in vivo imaging of PEG-poly(L-lysine)-based polymeric micelle MRI contrast agents, J. Control. Release (2009), doi:10.1016/j.jconrel.2009.01.010

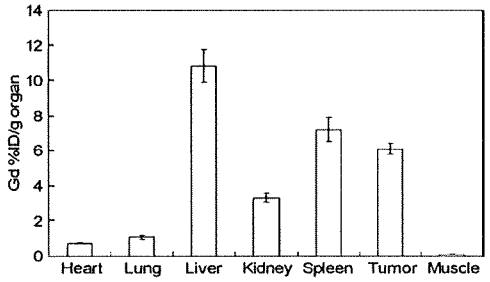

Fig. 5. Biodistribution of PEG-P(Lys-DOTA-Gd) micelle 24 h after injection at a dose of 0.05 mmol Gd/kg.

observations. The blood concentrations of the polymeric micelles were measured by means of ICP. Fig. 4 shows the blood concentration-time course of the polymeric micelles until 48 h after the injection. A low-molecular-weight gadolinium ion complex, such as Gd–DTPA, was immediately excreted 1 h after injection (only 1.4±0.8% was found in blood). On the other hand, the polymeric micelle remained 22.5±2.9% and 10.2±1.4% (mean±SD) in blood at 24 h and 48 h after the injection, respectively. These high blood concentrations exhibit significantly stable circulation of the polymeric micelle in blood. This polymeric micelle underwent an approximately 10-fold dilution relative to the injection in blood: however, stable formation of the polymeric micelle at such diluted conditions was confirmed in this in vivo experiment. This stable blood-circulation time-course was similar to the system of anti-cancer drug-incorporating polymeric micelle, a doxorubicin-incorporating poly(ethylene glycol)-*b*-poly (aspartic acid) system [1]. According to reports, the doxorubicin-incorporating polymeric micelle system provides a drug concentration of 24.6% of the injected dose (ID) after 24 h in the blood. Such a long circulating property of the doxorubicin-incorporating polymeric micelle successfully led to highly selective tumor accumulation. Owing to this similar pharmacokinetic behavior, this MRI contrast agent can be a strong tool for estimation of the pharmacokinetic behavior of "anti-cancer drug"-incorporating polymeric micelles.

3.3. Biodistribution and excretion of the polymeric micelle MRI contrast agent

Selective and high accumulation of drug carriers at solid tumors is essential for an improvement of anticancer drug efficacy. As well as the drug-targeting systems, selective and high accumulation is desired for diagnostic agents.

In recent decades, polymeric micelles have constituted one of the best drug-carriers to have achieved selective accumulation of an anti-cancer drug, through the EPR effect, at solid tumor tissues [1]. Biodistribution of the polymeric micelle contrast agents was evaluated in CDF_1 female mice bearing the colon 26 tumor. Fig. 5 shows the percentage of the injected dose of the polymeric micelle 24 h after the injection in the normal organs as well as in tumor tissues. The study showed that the accumulation of the polymeric micelle contrast agent in tumor tissues reached 6.1±0.3% ID (injected dose)/g of tumor. This accumulation amount was considerably high. Furthermore, highly selective delivery was present with low accumulation amounts in heart, kidney, and muscle tissue. For the mononuclear phagocyte system (MPS), this contrast agent was found to be accumulated in 10.8±0.9 and 7.2±0.7% ID/g of liver and spleen, respectively. These accumulation ratios were similar to those in case of doxorubicin-incorporated polymeric micelle, but better tumor/muscle ratios were obtained in this MRI contrast agent [1]. This difference may rest on a difference in micelle size as well as in detection species: there is a physically entrapped drug for the drug-carrying micelles and there are chelated gadolinium ions for the MRI contrast agent. The gadolinium-binding macromolecular carrier may

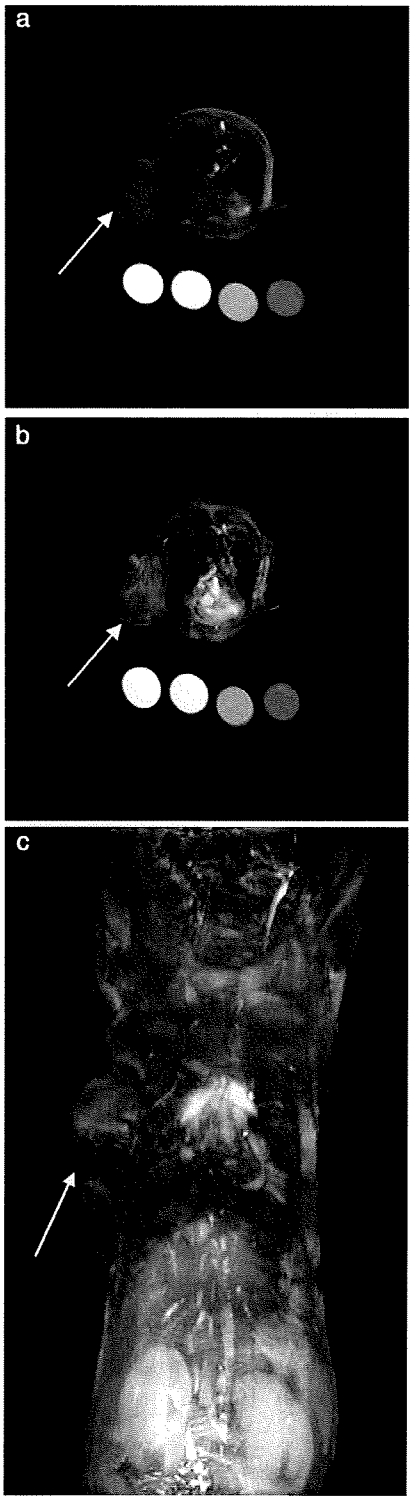

Fig. 6. Axial slices of MR images (a) before and (b) 24 h after the injection at a dose of 0.05 mmol Gd/kg. Tumor areas are on the left side in the axial slices. The circles indicate the stock solutions of (left to right) 1.0 mM, 0.5 mM, 0.1 mM gadolinium ion in agarose gel and blank in agarose gel. T_1-weighted gradient echo protocol was used. Parameters of the T_1-weighted images were TR/TE=8.0/4.5, flip angle=30°, field of view of 45×45 mm, a matrix size of 192×192, and 2 mm of axial slice thickness. Arrows indicate tumor tissue. (c) MIP images of coronal slices 24 h after injection. Arrow indicates tumor. Parameters of the T_1-weighted images were TR/TE=8.0/4.2, flip angle=30°, field of view of 50×30 mm, a matrix size of 192×192. MIP images were obtained by 2 mm thickness×4 slices.

Please cite this article as: K. Shiraishi, et al., Preparation and in vivo imaging of PEG-poly(L-lysine)-based polymeric micelle MRI contrast agents, J. Control. Release (2009), doi:10.1016/j.jconrel.2009.01.010

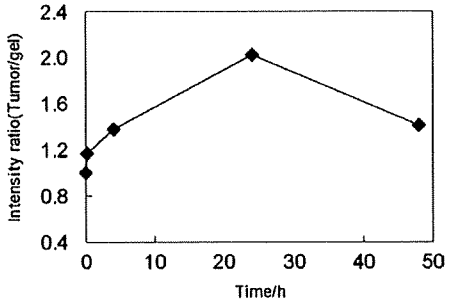

Fig. 7. Relative signal intensities of tumor area at defined time (0 h, 4 h, 24 h, 48 h) after the injection of the polymeric micelle MRI contrast agent.

not penetrate into muscle as do low-"molecular weight" drugs that are released from the carrier.

Wang Y et al. reported that poly[N-(2-hydroxypropyl)methacrylamide] (PHPMA) [14] gadolinium-conjugates exhibited size-dependent tumor accumulation. They stated that a large molecular weight of PHPMA (121 kDa) gadolinium conjugate exhibited the best tumor accumulation at 7 days after injection. Although, Bogdanov A et al. reported another example of successful passive targeting to solid tumors with a graft copolymer of poly(ethylene glycol) featuring poly(L-lysine) [9]. This contrast agent exhibited tumor targeting with a long blood-circulation time ($t_{1/2}$=36 h): however, this long-circulation property in blood indicates that the contrast agent cannot excrete smoothly from the body owing to the polymer's very large molecular weight (690 kDa). The researchers synthesized different molecular weights of similar polymers to compare the polymers' biodistribution [10] and found that the polymers accumulated at solid tumors in a "molecular-weight"-dependent manner. This molecular-weight dependency indicated that smaller molecular weights of polymers can be excreted through the kidneys.

These above-mentioned polymers exhibited better tumor accumulation, corresponded to larger molecular weights of the polymers. However, the excretion of the contrast agent, especially in the case of the macromolecular contrast agent, is a serious matter for the development of diagnostic agents.

Therefore, we checked the kidneys' excretion of our polymeric micelle contrast agent. In urine, 20.8±7.6% of the polymeric micelle was found 48 h after the injection. This result indicates that the polymeric micelle was excreted through the kidney filtration. Since the size of the polymeric micelle contrast agent was 50–250 nm as shown in Fig. 3(a), the polymeric micelles cannot pass through the kidney filtration. Therefore, these polymers that formed in urine appears to have passed through the kidney filtration in a dissociated polymer form, since the average molecular weight of this block copolymer is only 15,000. This is an excellent property of the polymeric micelle MRI contrast agent; namely, this agent exhibits long circulation in blood in a micelle form, while this agent can be excreted through the kidneys in a dissociated polymer form.

Furthermore, the obtained polymeric micelle MRI contrast agent delivered a larger amount to solid tumors than did previously reported macromolecular MRI contrast agents that can be also excreted from the kidneys (agents such as PHPMA gadolinium-conjugate [14] and graft copolymer of poly(ethylene glycol) with poly (L-lysine) [10]).

In order to estimate possible acute toxicity, we injected the 4-fold of the volume of the contrast agent into the mouse tail vein, and observed the body weight change over the course of 16 days. There was no significant difference in comparison to the control (less than ±10%). Although we have to conduct further experiments to obtain toxicity-related information of greater exactness, these preliminary results indicate that this polymeric micelle can dissociate and be excreted from the kidneys, and that this tumor targeting results a passive targeting mechanism (the EPR effect). In a future study, we would like to optimize the pharmacokinetics and the dissociation behavior of the polymeric micelles by controlling the composition of the block copolymers.

3.4. MR imaging at tumor tissue

We took an MR image of the tumor-bearing mouse after the injection of the polymeric micelle contrast agent. Fig. 6 shows T_1-weighted MR images of tumor tissues before and after 24 h at an injection dose of 0.05 mmol Gd/kg. After the injection of the polymeric micelle, MR images exhibited a significant signal enhancement at the kidneys. This signal enhancement at the kidneys indicates that kidneys excreted the contrast agent, as shown in Fig. 6(c). However, even 24 h after the injection, an intense signal was observed in the heart and aorta areas. This indicates that a considerable amount of the contrast agent was circulating in the bloodstream, as described in pharmacokinetic results. The relative signal intensity at axial slices of the tumor tissues underwent a 2.0-fold increase after 24 h, as compared with the signal before the injection. The signal intensity of the tumor area had gradually increased by 24 h and had slightly decreased by 48 h, as shown in Fig. 7. This behavior of the signal intensities is similar to the doxorubicin concentration delivered by the polymeric micelle carrier system. All these results indicate that the enhancement of MR signals in the tumor area rested on the successful passive accumulation of the MRI contrast agent at solid tumors.

4. Conclusion

We prepared polymeric micelle MRI contrast agents using poly (ethylene glycol)-*b*-poly(L-lysine) block copolymers. A reaction of poly(ethylene glycol)-*b*-poly(L-lysine) with a DOTA derivative resulted in a quantitative DOTA conjugation regarding the lysine residues of the block copolymer, and the obtained block copolymer formed a polymeric micelle. This micellar structure was maintained after a partial chelation of the DOTA moiety with gadolinium ions. The biodistribution and the excretion of the polymeric micelle was evaluated in colon 26-bearing CDF_1 female mice. Selective accumulation of the polymeric micelle at the tumor tissues was observed 24 h after the injection. The contrast agent's accumulation substantially enhanced the signal intensity of the MR images at the tumor. This polymeric micelle MRI contrast agent will be a useful diagnostic tool, particularly in combination with a polymeric micelle-based drug-targeting system.

Acknowledgement

This work was supported by the Ministry of Health, Labour, and Welfare of Japan. K. Shiraishi and M. Yokoyama acknowledge the support from the Program for Promoting the Establishment of Strategic Research Centers, Special Coordination Funds for Promoting Science and Technology, the Ministry of Education, Culture, Sports, Science and Technology of Japan, and Tokyo Ohka Foundation for the Promotion of Science and Technology.

Appendix A. Supplementary data

Supplementary data associated with this article can be found, in the online version, at doi:10.1016/j.jconrel.2009.01.010.

References

[1] M. Yokoyama, T. Okano, Y. Sakurai, S. Fukushima, K. Okamoto, K. Kataoka, Selective delivery of adriamycin to a solid tumor using a polymeric micelle carrier system, J. Drug Target. 7 (3) (1999) 171–186.

[2] Y. Matsumura, H. Maeda, A new concept for macromolecular therapeutics in cancer chemotherapy: mechanism of tumoritropic accumulation of proteins and the antitumor agent Smancs, Cancer Res. 46 (1986) 6387–6392.
[3] H.M. Aliabadi, A. Lavasanifar, Polymeric micelles for drug delivery, Expert Opin. Drug Deliv. 3 (1) (2006) 130–162.
[4] N. Nishiyama, S. Okazaki, H. Cabral, M. Miyamoto, Y. Kato, Y. Sugiyama, K. Nishio, Y. Matsumura, K. Kataoka, Novel cisplatin-incorporated polymeric micelles can eradicate solid tumors in mice, Cancer Res. 63 (2003) 8977–8983.
[5] N. Nishiyama, M. Yokoyama, T. Aoyagi, T. Okano, Y. Sakurai, K. Kataoka, Preparation and characterization of self-assembled polymer–metal complex micelle from cis-dichlorodiammineplatinum(II) and poly(ethylene glycol)-poly(α,β-aspartic acid) block copolymer in an aqueous medium, Langmuir 15 (1999) 377–383.
[6] A. Bogdanov Jr, C. Martin, A.V. Bogdanova, T.J. Brady, R. Weissleder, An adduct of cis-diamminedichloroplatinum(II) and poly(ethylene glycol)poly(L-lysine)-succinate: synthesis and cytotoxic properties, Bioconjug. Chem. 7 (1) (1996) 144–149.
[7] R. Rebizak, M. Schaefer, E. Dellacherie, Polymeric conjugates of Gd^{3+}-diethylenetriaminepentaacetic acid and dextran. 1. Synthesis, characterization, and paramagnetic properties, Bioconjug. Chem. 8 (4) (1997) 605–610.
[8] M.M. Huber, A.B. Staubli, K. Kustedjo, M.H.B. Gray, J. Shih, S.E. Fraser, R.E. Jacobs, T.J. Meade, Fluorescently detectable magnetic resonance imaging agents, Bioconjug. Chem. 9 (2) (1998) 242–249.
[9] A. Bogdanov Jr, S.C. Wright, E.M. Marecos, A.V. Bogdanova, C. Martin, R. Weissleder, A long-circulating co-polymer in "passive targeting" to solid tumors, J. Drug Target. 4 (5) (1997) 321–330.
[10] R. Weissleder, A. Bogdanov Jr, C-H. Tung, H-J. Weinmann, Size optimization of synthetic graft copolymers for in vivo angiogenesis imaging, Bioconjug. Chem. 12 (2) (2001) 213–219.
[11] F. Ye, T. Ke, E-K. Jeong, X. Wang, Y. Sun, M. Johnson, Z-R. Lu, Noninvasive visualization of in vivo drug delivery of poly(L-glutamic acid) using contrast-enhanced MRI, Mol. Pharm. 3 (5) (2006) 507–515.
[12] X. Wen, E.F. Jackson, R.E. Price, E.E. Kim, Q. Wu, S. Wallace, C. Charnsangavej, J.G. Gelovani, C. Li, Synthesis and characterization of poly(L-glutamic acid) gadolinium chelate: a new biodegradable MRI contrast agent, Bioconjug. Chem. 15 (6) (2004) 1408–1415.
[13] Z-R. Lu, X. Wang, D.L. Parker, K.C. Goodrich, H.R. Buswell, Poly(L-glutamic acid) Gd (III)–DOTA conjugate with a degradable spacer for magnetic resonance imaging, Bioconjug. Chem. 14 (4) (2003) 715–719.
[14] Y. Wang, F. Ye, E-K. Jeong, Y. Sun, D.L. Parker, Z-R. Lu, Noninvasive visualization of pharmacokinetics, biodistribution, and tumor targeting of poly[N-(2-hydroxypropyl)methacrylamide] in mice using contrast enhanced MRI, Pharm. Res. 24 (6) (2007) 1208–1216.
[15] H. Kobayashi, M.W. Brechbiel, Dendrimer-based macromolecular MRI contrast agents: characterization and application, Mol. Imag. 2 (1) (2003) 1–10.
[16] H. Kobayashi, S. Kawamoto, S-K. Jo, H.L. Bryant Jr, M.W. Brechbiel, R.A. Star, Macromolecular MRI contrast agents with small dendrimers: pharmacokinetic differences between sizes and cores, Bioconjug. Chem. 14 (2) (2003) 388–394.
[17] H. Kobayashi, N. Sato, S. Kawamoto, T. Saga, A. Hiraga, T.L. Haque, T. Ishimori, J. Konishi, K. Togashi, M.W. Brechbiel, Comparison of the macromolecular MR contrast agents with ethylenediamine-core versus ammonia-core generation-6 polyamidoamine dendrimer, Bioconjug. Chem. 12 (1) (2001) 100–107.
[18] E. Nakamura, K. Makino, T. Okano, T. Yamamoto, M. Yokoyama, A polymeric micelle MRI contrast agent with changeable relaxivity, J. Control. Release 114 (2006) 325–333.
[19] V.P. Torchilin, PEG-based micelles as carriers of contrast agents for different imaging modality, Adv. Drug Deliv. Rev. 54 (2002) 235–252.
[20] G. Zhang, R. Zhang, X. Wen, L. Li, C. Li, Micelles based on biodegradable poly(L-glutamic acid)-b-polylactide with paramagnetic Gd ions chelated to the shell layer as a potential nanoscale MRI-visible delivery, Biomacromolecules 9 (1) (2008) 36–42.
[21] H.Y. Lee, H.W. Jee, S.M. Seo, B.K. Kwak, G. Khang, S.H. Cho, Diethylenetiramine-pentaacetic acid–gadolinium (DTPA–Gd)-conjugated polysuccinimide derivatives as magnetic resonance imaging contrast agents, Bioconjug. Chem. 17 (3) (2006) 700–706.
[22] N. Nasongkla, E. Bey, J. Ren, H. Ai, C. Khemtong, J.S. Guthi, S-F. Chin, A.D. Sherry, D.A. Boothman, J. Gao, Multifunctional polymeric micelles as cancer-targeted, MRI-ultrasensitive drug delivery systems, Nano Lett. 6 (11) (2006) 2427–2430.
[23] Z-R. Lu, F. Ye, A. Vaidya, Polymer platforms for drug delivery and biomedical imaging, J. Control. Release 122 (2007) 269–277.
[24] M. Yokoyama, G.S. Kwon, T. Okano, Y. Sakurai, M. Naito, K. Kataoka, Influencing factors on in vitro micelle stability of adriamycin-block copolymer conjugate, J. Control. Release 28 (1994) 59–65.
[25] Y. Takakura, T. Fujita, M. Hashida, H. Sezaki, Disposition character of macromolecules in tumor-bearing mice, Pham. Res. 7 (4) (1990) 330–346.
[26] A. Harada, K. Kataoka, Formation of polyion complex micelles in an aqueous milieu from a pair of oppositely-charged block copolymers with poly(ethylene glycol) segments, Macromolecules 28 (15) (1995) 5294–5299.

Please cite this article as: K. Shiraishi, et al., Preparation and in vivo imaging of PEG-poly(L-lysine)-based polymeric micelle MRI contrast agents, J. Control. Release (2009), doi:10.1016/j.jconrel.2009.01.010

International Journal of Pharmaceutics 373 (2009) 100–106

Contents lists available at ScienceDirect

International Journal of Pharmaceutics

journal homepage: www.elsevier.com/locate/ijpharm

Pharmaceutical Nanotechnology

Enhanced *in vivo* antitumor efficacy of fenretinide encapsulated in polymeric micelles

Tomoyuki Okuda[a], Shigeru Kawakami[a], Yuriko Higuchi[a], Taku Satoh[b], Yoshimi Oka[b], Masayuki Yokoyama[b], Fumiyoshi Yamashita[a], Mitsuru Hashida[a,c,*]

[a] *Department of Drug Delivery Research, Graduate School of Pharmaceutical Sciences, Kyoto University, Sakyo-ku, Kyoto 606-8501, Japan*
[b] *Kanagawa Academy of Science and Technology, KSP East 404, Sakado 3-2-1, Takatsu-ku, Kawasaki-shi, Kanagawa 213-0012, Japan*
[c] *Institute of Integrated Cell-Material Sciences (iCeMS), Kyoto University, Yoshida, Sakyo-ku, Kyoto 606-8501, Japan*

ARTICLE INFO

Article history:
Received 3 October 2008
Received in revised form 21 January 2009
Accepted 23 January 2009
Available online 31 January 2009

Keywords:
Fenretinide
4-HPR
Retinoid
Polymeric micelle
Controlled release
Drug delivery system

ABSTRACT

Fenretinide (N-(4-hydroxyphenyl)retinamide, 4-HPR) is a synthetic retinoid with high antitumor activity against a variety of malignant cells *in vitro*, and is a promising candidate for cancer chemoprevention and chemotherapy. To enhance the antitumor efficacy of 4-HPR *in vivo*, 4-HPR were encapsulated into polymeric micelles for tumor targeting by enhanced permeability and retention effects. 4-HPR encapsulated in poly(ethylene glycol)–poly(benzyl aspartate) block copolymer micelles were prepared by the evaporation method. The mean particle size of 4-HPR encapsulated in polymeric micelles was about 173 nm. After intravenous injection into tumor-bearing mice, the delivery of 4-HPR by polymeric micelles increased the blood concentration and enhanced the tumor accumulation of 4-HPR over the injection of the 4-HPR encapsulated in oil-in-water (O/W) emulsions. Tumor growth was significantly delayed following treatment by 4-HPR encapsulated in polymeric micelles, which demonstrated the improved *in vivo* antitumor efficacy of 4-HPR. In addition, 4-HPR encapsulated in polymeric micelles did not cause any body weight loss. These results suggest that polymeric micelles are a promising and effective carrier of 4-HPR in order to enhance tumor delivery and have potential application in the treatment of solid tumor.

1. Introduction

Retinoids are a class of natural or synthetic derivatives of vitamin A that exert various biological actions on cellular growth and differentiation (Means and Gudas, 1995; Kagechika and Shudo, 2005). As a result of their unique characteristics, their application in novel cancer therapy has been progressing (Altucci and Gronemeyer, 2001; Clarke et al., 2004). In particular, fenretinide (N-(4-hydroxyphenyl)retinamide, 4-HPR), which was synthesized from all-trans retinoic acid (ATRA), is a promising candidate for cancer chemoprevention and chemotherapy, since it has higher antitumor activity and lower toxicity than other retinoids (Moon et al., 1979; Miller, 1998). It was reported that the antitumor activity of 4-HPR was through two main mechanisms: retinoic acid receptor-dependent cascade and retinoic acid receptor-independent cascade, including reactive oxygen species generation, ceramide synthesis, and proapoptotic bcl-2 family protein (Bax and Bak) induction (Hail et al., 2006; Corazzari et al., 2005). Clinical trials of 4-HPR have been progressing against breast cancer, prostate cancer, and neuroblastoma (Altucci and Gronemeyer, 2001; Clarke et al., 2004).

To date, 4-HPR has been clinically administrated using an oral gelatin capsule containing 4-HPR in corn oil and polysorbate 80 [available through the National Cancer Institute]; however, this formulation has poor bioavailability, since 4-HPR itself is too hydrophobic to pass through intestinal membrane easily (Kokate et al., 2007), and requires excessive or multiple administrations to achieve a higher blood concentration of 4-HPR (Villablanca et al., 2006). In addition, several animal studies have demonstrated that intravenously injected 4-HPR is rapidly eliminated from the body (Swanson et al., 1980; Hultin et al., 1986); therefore, the development of a targeted carrier of 4-HPR is needed to exert *in vivo* antitumor efficacy.

Polymeric micelles are a class of micelles that are formed from block copolymers typically consisting of hydrophilic and hydrophobic polymer chains (Kataoka et al., 2001; Torchilin, 2004). They are of particular interest because of their efficacy in entrapping a satisfactory amount of hydrophobic drugs within the inner core, their stability in the circulation and their ability to gradually release the drugs (Kwon, 2003). In addition, the highly hydrated outer

* Corresponding author at: Department of Drug Delivery Research, Graduate School of Pharmaceutical Sciences, Kyoto University, Sakyo-ku, Kyoto 606-8501, Japan. Tel.: +81 75 753 4525; fax: +81 75 753 4575.
E-mail address: hashidam@pharm.kyoto-u.ac.jp (M. Hashida).

0378-5173/$ – see front matter © 2009 Published by Elsevier B.V.
doi:10.1016/j.ijpharm.2009.01.019

shells of the micelles prevent reticuloendothelial system (RES) uptake and inhibit intermicellar aggregation of their hydrophobic inner cores. The characteristics of these polymeric micelles could be an advantage for passive delivery and to extravasate the drug at tumor sites by enhanced permeability and retention (EPR) effects (Maeda, 2001). In our previous report, we demonstrated that poly(ethylene glycol)–poly(aspartate) block copolymer micelles modified with benzyl groups could stably encapsulate 4-HPR and enhanced blood retention of 4-HPR after intravenous injection into mice (Okuda et al., 2008). This observation prompted us to investigate the potential use of polymeric micelles to enhance tumor retention and *in vivo* antitumor efficacy of 4-HPR in tumor-bearing mice.

In this study, we extended our previous study and tumor distribution and antitumor efficacy of 4-HPR encapsulated in poly(ethylene glycol)–poly(aspartate) block copolymer micelles modified with benzyl groups after intravenous injection were examined in mice bearing murine melanoma B16BL6 tumors. As a control pharmaceutical formulation of 4-HPR, oil-in-water (O/W) or PEGylated O/W emulsions were selected because of their preparation characteristics for delivery of highly lipophilic drugs (Tamilvanan, 2004).

2. Materials and methods

2.1. Materials

4-HPR was purchased from Tokyo Chemical Industry, Co. Ltd. (Tokyo, Japan). Egg yolk phosphatidylcholine (EggPC) and 3-(4,5-dimethyl-2-thiazoyl)-2,5-diphenyl-2H tetrazolium bromide (MTT) were purchased from Sigma–Aldrich (St. Louis, MO, USA). Soybean oil (SO) and ATRA were purchased from Wako Pure Chemicals Industry, Ltd. (Osaka, Japan). Acetonitrile (HPLC grade) and acetic acid (HPLC grade) were purchased from Nacalai Tesque, Inc. (Kyoto, Japan). Distearoylphosphatidylethanolamine-N-[methoxy(polyethylene glycol)-2000] (PEG-DSPE) was purchased from Nippon Oil and Fats Co. (Tokyo, Japan). Fetal bovine serum (FBS) was obtained from Biowhittaker (Walkersville, MD). Dulbecco's modified Eagle's medium (DMEM), phosphate-buffered saline (PBS), and Hank's balanced saline solution (HBSS) were purchased from Nissui Pharmaceutical Co., Ltd. (Tokyo, Japan). All other chemicals were of the highest purity available.

2.2. Synthesis of block copolymer

Poly(ethylene glycol)–poly(aspartic acid) (PEG–P(Asp)) block copolymer was obtained by alkaline hydrolysis of poly(ethylene glycol)–poly(β-benzyl-L-aspartate) (PEG–PBLA), as reported previously (Opanasopit et al., 2004). Briefly, the molecular weight of poly(ethylene glycol) (PEG) chain was 5000 and the average number of aspartic acid units was 27. Approximately 75% of the aspartic acid residues in poly(aspartic acid) chain were converted to the β-amide form by alkaline hydrolysis during the synthesis of this block copolymer. A hydrophobic benzyl group was bound to 77% of the poly(aspartic acid) residues by an ester-forming reaction between benzyl bromide and PEG–P(Asp), as reported previously (Yokoyama et al., 2004). Briefly, PEG–P(Asp) block copolymer was dissolved in N,N-dimethylformamide (DMF) and added to benzyl bromide along with a catalyst, 1,8-diazabicyclo[5,4,0]7-undecene (DBU). The reaction mixture was stirred at 50 °C for 15.5 h. Polymer was obtained by precipitation in excess of diethyl ether and collected by filtration. The dried polymer was dissolved in dimethyl sulfoxide (DMSO), and then 6N HCl was added, followed by dialysis against distilled water and finally, freeze-drying.

For determination of the polymer composition, such as the number of aspartic acid units and the benzyl ester content, ^{1}H NMR measurements were carried out on a 1% solution in 6D-DMSO containing 3% trifluoroacetic acid using a Varian Unity Inova NMR spectrometer at 400 MHz.

2.3. Preparation of 4-HPR encapsulated in polymeric micelles

4-HPR encapsulated in polymeric micelles was prepared by a conventional evaporation method (Kawakami et al., 2005; Chansri et al., 2008). Briefly, 4-HPR and polymer were dissolved in chloroform. After vacuum drying and desiccation, PBS (pH 7.4) was added for suspension in a bath sonicator for 3 min. The suspension was sonicated for 3 min (200 W) at 75 °C using a probe sonicator (US 300, Nissei, Inc., Tokyo, Japan). The preparation was centrifuged at 1400 × *g* for 10 min before the supernatant was passed through a 0.45 μm filter.

2.4. Preparation of 4-HPR encapsulated in O/W emulsions and PEGylated O/W emulsions

4-HPR encapsulated in O/W emulsions was prepared based on our previous reports (Takino et al., 1994; Chansri et al., 2006). Briefly, 4-HPR, EggPC, and SO (30:150:150, weight ratio) were dissolved in chloroform. After vacuum drying and desiccation, PBS (pH 7.4) was added for suspension in a bath sonicator for 3 min. The suspension was sonicated for 30 min (200 W) at 4 °C using a probe sonicator (US 300, Nissei, Inc., Tokyo, Japan). 4-HPR encapsulated in PEGylated O/W emulsions, composed of 4-HPR, EggPC, PEG-DSPE, and SO (30:105:45:150, weight ratio), was also prepared using this protocol.

2.5. Characterization of the formulations

The concentration of 4-HPR in the preparations was determined by UV absorption at 370 nm (UV–vis Spectrophotometer, Shimazu Co. Ltd., Kyoto, Japan) after dissolving in DMSO (the preparations: DMSO = 10:990, volume ratio). The recovery of 4-HPR was calculated from the concentration of 4-HPR in the preparations (C_P) as follows:

$$\text{Recovery}(\%) = \frac{C_P(\text{mg/mL}) \times \text{added PBS(mL)}}{\text{initial amount of 4-HPR(mg)}} \times 100$$

On the other hand, the recovery of polymer was defined as 100% because of high solubility of polymer in PBS (>50 g/L). The particle sizes and polydispersion indexes of the preparations were measured by Zetasizer Nano Series (Malvern Instruments Ltd., Worcestershire, UK).

2.6. Animals

Male C57BL/6 mice (4 weeks old, 14–19 g) were purchased from the Shizuoka Agricultural Cooperative Association for Laboratory Animals (Shizuoka, Japan). Animals were maintained under conventional housing conditions. All animal experiments were carried out in accordance with the guidelines for Animal Experiments of Kyoto University.

2.7. Tumor cells

Murine melanoma B16BL6 cells were obtained from the Cancer Chemotherapy Center of the Japanese Foundation for Cancer Research (Tokyo, Japan). They were grown in DMEM supplemented with 10% heat-inactivated FBS, 0.15% $NaHCO_3$, 100 units/mL penicillin, and 100 μg/mL streptomycin at 37 °C in humidified air containing 5% CO_2.

2.8. MTT assay

MTT assay was performed by the method described previously (Kawakami et al., 2006). B16BL6 cells were placed on a 96-well cluster dish at a density of 3×10^3 cells/0.28 cm^2. Twenty-four hours later, medium containing various concentrations of 4-HPR, empty polymeric micelles, and 4-HPR encapsulated in polymeric micelles was added to the plates. At each exposure time point, the medium was removed and 5 mg/mL MTT solution was added to each well. Cells were incubated for 4 h at 37 °C in 5% CO_2 and then 10% sodium dodecyl sulfate (SDS) solution was added, followed by incubation overnight to dissolve formazan crystals. An absorbance was measured at wavelengths of 570 nm in a microplate photometer (Bio-Rad Model 550, Bio-Rad Laboratories, Inc., Hercules, CA, USA). IC_{50} values were determined from dose-response curves by a nonlinear regression analysis using MULTI program developed by Yamaoka et al. (Yamaoka et al., 1981) and represent the concentration required to inhibit cell viability by 50%.

2.9. Tumor-bearing mouse model

After harvesting by trypsin, B16BL6 cells were prepared at a concentration of 4×10^6 cells/mL by HBSS. Then, 0.05 mL of the cell suspension (2×10^5 cells) was inoculated subcutaneously in the lower back of each C57BL/6 mouse. A solid tumor was observed within 7 days after tumor inoculation.

2.10. In vivo distribution study

4-HPR encapsulated in polymeric micelles, O/W emulsions, and PEGylated O/W emulsions were adjusted to 7.5 mg/mL as 4-HPR. On 14 days after tumor inoculation, they were intravenously injected into the tail vein of B16BL6-bearing mice at a dose of 75 mg/kg as 4-HPR. At each collection time point, blood was collected from the vena cava under anesthesia, and mice were killed for tumor excision. Blood was centrifuged at 5000 × *g* for 5 min at 4 °C before 200 μL of plasma was collected. The plasma was added to 400 μL of acetonitrile and 4 μL of 2 mg/mL ATRA (dissolved in ethanol) as an internal standard and vortexed. Part 0.2 g of the excised tumor was collected and added to 500 μL of acetonitrile and 5 μL of 2 mg/mL ATRA, followed by sonication using a bath sonicator for 15 min. The extract from plasma and tumor was centrifuged at 13,000 × *g* for 3 min at 4 °C, and the supernatant was collected and passed through a 0.45 μm filter. The filtrated extract was analyzed by HPLC.

2.11. HPLC conditions

The extract was analyzed with a high-performance liquid chromatograph device, consisting of a system controller (SLC-10A VP, Shimazu Co. Ltd., Kyoto, Japan), a UV–vis detector (SPD-10A VP, Shimazu Co. Ltd., Kyoto, Japan), an auto injector (SIL-10A, Shimazu Co. Ltd., Kyoto, Japan), and a HPLC pump (LC-10AS, Shimazu Co. Ltd., Kyoto, Japan). The UV–vis detector was set at 350 nm. A C18 reverse-phase column (ODS-A 150 mm × 4.6 mm, YMC Co. Ltd., Kyoto, Japan) was used. The mobile phase consisted of acetonitrile:water:acetic acid (80:19:1, volume ratio) delivered at a flow rate of 1 mL/min. The injection volume was 50 μL. All samples were analyzed at room temperature.

2.12. Pharmacokinetic analysis

Pharmacokinetic parameters including the half-life ($t_{1/2}$), the area under the concentration versus time curve ($AUC_{t-\infty}$), the total body clearance (CL_{tot}), the volume of distribution at steady state (V_{dss}), and the mean residence time (MRT) were all calculated by moment analysis program developed by Yamaoka et al. (1978).

2.13. In vivo antitumor efficacy in tumor-bearing mice

On 8 days after tumor inoculation when the tumor volume reached approximately 100 mm^3, each treatment was started. 4-HPR encapsulated in polymeric micelles and O/W emulsions was intravenously injected into the tail vein of B16BL6-bearing mice at a dose of 75 mg/(kg day) as 4-HPR. The dose of empty polymeric micelles was 375 mg/(kg day) as polymer, which was an equivalent does to 4-HPR encapsulated in polymeric micelles. In the control groups, PBS was administrated. Each treatment was performed at 10 mL/(kg day) on 8, 10, and 12 days after tumor inoculation. Tumor diameter and body weight were measured for each mouse at 2-day intervals after the treatment started. Tumor volume was calculated as follows:

$$\text{Tumor volume} = \frac{\pi}{6} \times LW^2$$

where L is the long diameter and W is the short diameter.

2.14. Statistical analysis

Statistical comparison was performed by Student's *t*-test for two groups, and Dunnett's test for multiple groups. $P < 0.05$ was considered significant.

3. Results

3.1. Characteristics of 4-HPR encapsulated in polymeric micelles

Poly(ethylene glycol)–poly(benzyl aspartate) block copolymer was successfully synthesized from PEG–P(Asp), and about 77% of the aspartic residues were esterified with benzyl groups as reported previously (Opanasopit et al., 2004). The recovery of 4-HPR achieved approximately 70% in polymer/4-HPR weight ratio at 2.5 and 3.0 (Fig. 1). Therefore, polymer/4-HPR weight ratio was fixed at 2.5 in the following experiments. The mean particle size of polymeric micelles was about 173 nm (Fig. 2). On the other hand, the mean particle sizes of O/W emulsions and PEGylated O/W emulsions were about 176 and 178 nm, respectively, similar to polymeric micelles. The polydispersion indexes of polymeric micelles, O/W

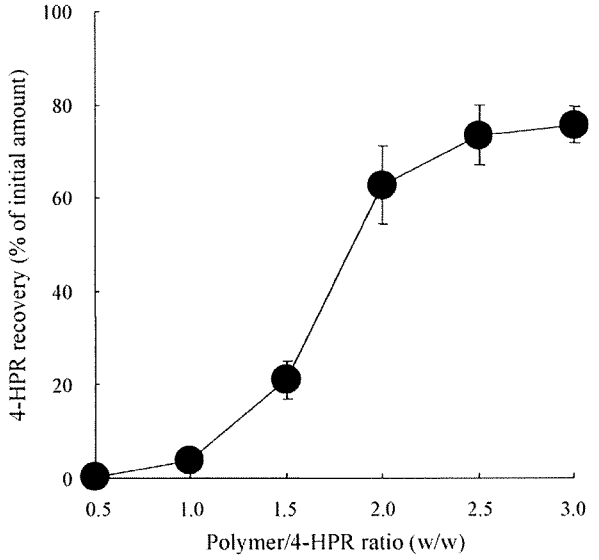

Fig. 1. Effect of polymer/4-HPR weight ratio on encapsulation of 4-HPR into prepared polymeric micelles. 4-HPR encapsulated in polymeric micelles was prepared at various weight ratio for 1 mg 4-HPR, and 4-HPR recovery was calculated. Each value represents the mean ± S.D. ($n = 4$).

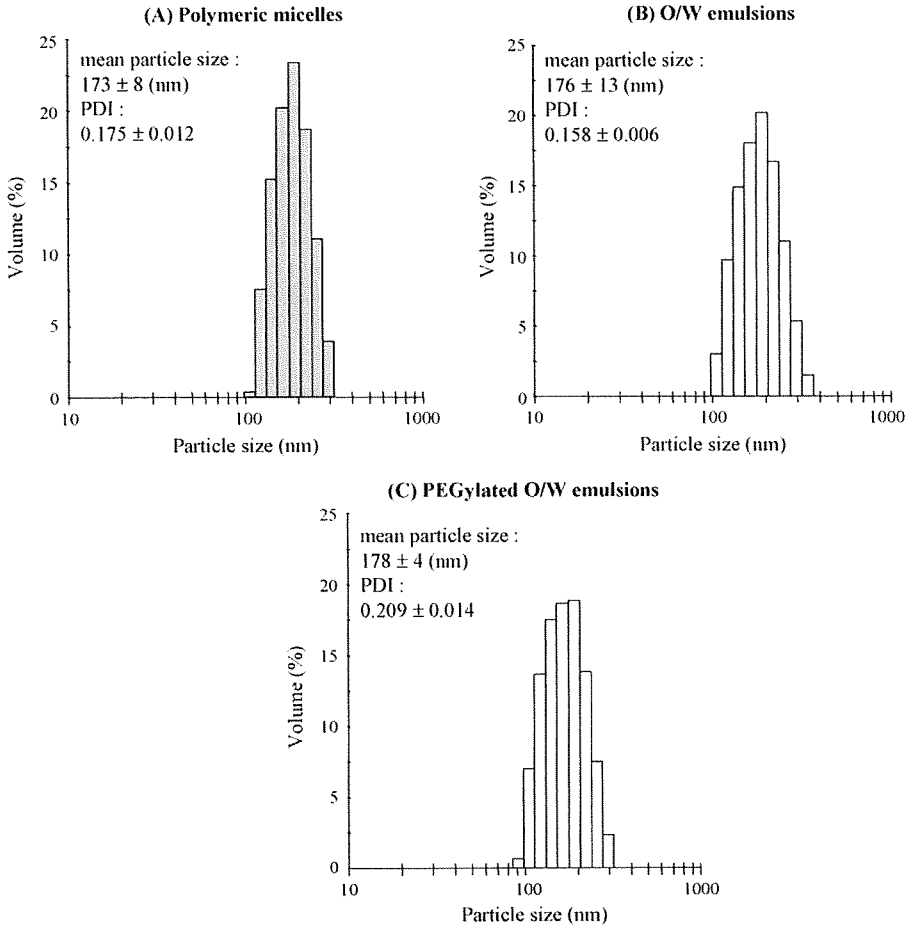

Fig. 2. Size distributions, mean particle sizes, and polydispersion indexes (PDI) of 4-HPR encapsulated in polymeric micelles (A), 4-HPR encapsulated in O/W emulsions (B), and 4-HPR encapsulated in PEGylated O/W emulsions (C). Each value of represents the mean ± S.D. ($n = 3$).

emulsions, and PEGylated O/W emulsions were about 0.175, 0.158, and 0.209, respectively, suggesting the narrow size distribution of these preparations. Furthermore, the particle size of 4-HPR encapsulated in polymeric micelles remained constant over 1 month at room temperature, 4, and −30 °C (data not shown).

3.2. *In vitro antitumor activity of 4-HPR and 4-HPR encapsulated in polymeric micelles*

For evaluating *in vitro* antitumor activity of 4-HPR and 4-HPR encapsulated in polymeric micelles against B16BL6 cells, MTT assay was performed. The *in vitro* antitumor activity of 4-HPR was enhanced as the increase of dose and exposure time (Fig. 3(A)). IC_{50} value was settled on approximately 0.60 μg/mL at more than 24 h, suggesting full antitumor activity of 4-HPR could be obtained at 24 h. IC_{50} value of 4-HPR encapsulated in polymeric micelles (52 μg/mL at 48 h) was much larger than that of free form of 4-HPR (0.60 μg/mL at 48 h) (Fig. 3(B)). This result may indicate the stable encapsulation of 4-HPR into polymeric micelles in medium.

3.3. *Distribution of 4-HPR in tumor-bearing mice*

The blood concentration and tumor accumulation of 4-HPR after intravenous injection of 4-HPR encapsulated in polymeric micelles were evaluated in B16BL6-bearing mice (Fig. 4) and compared with those of 4-HPR encapsulated in O/W emulsions or PEGylated O/W emulsions as control. The blood concentration of 4-HPR encapsulated in polymeric micelles was significantly higher than those of 4-HPR encapsulated in O/W emulsions and PEGylated O/W emulsions, suggesting that polymeric micelles could enhance the blood retention of 4-HPR compared with O/W emulsions and PEGylated O/W emulsions. Moreover, the tumor accumulation of 4-HPR encapsulated in polymeric micelles was significantly higher and prolonged for 48 h compared with O/W emulsions and PEGylated O/W emulsions. Pharmacokinetic parameters of 4-HPR encapsulated in polymeric micelles, O/W emulsions, and PEGylated O/W emulsions were shown in Table 1. The area under the curve ($AUC_{0-\infty}$) in blood was approximately 23.9 times higher for 4-HPR encapsulated in polymeric micelles than for that in O/W emulsions. The $t_{1/2}$ in blood was approximately 5.02 times longer for 4-HPR encapsulated in polymeric micelles than for that in O/W emulsions. Furthermore, the maximum concentration (C_{max}), and the $AUC_{0-\infty}$ in tumors were approximately 3.03 and 16.9 times higher for 4-HPR encapsulated in polymeric micelles than for that in O/W emulsions, respectively. The $t_{1/2}$ in tumors was approximately 5.63 times longer for 4-HPR encapsulated in polymeric micelles than for that in O/W emulsions.

3.4. *In vivo antitumor efficacy of 4-HPR encapsulated in polymeric micelles in tumor-bearing mice*

In vivo antitumor efficacy of 4-HPR encapsulated in polymeric micelles was evaluated in B16BL6-bearing mice after intravenous injection of PBS (control), empty polymeric micelles, 4-HPR encapsulated in O/W emulsions, and 4-HPR encapsulated in polymeric micelles. Each treatment was performed on 8, 10, and 12 days (total

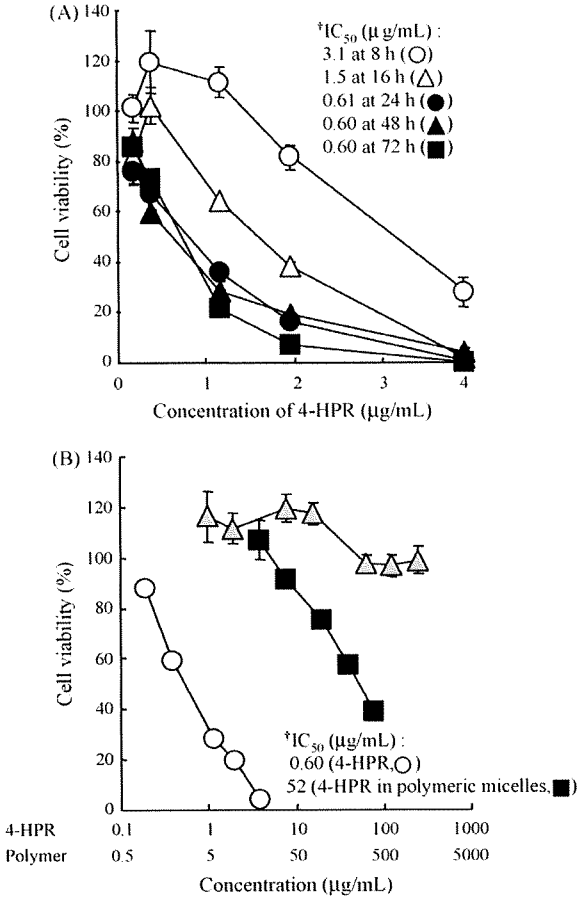

†IC_{50} values were determined from dose-response curves by a nonlinear regression analysis using MULTI program developed by Yamaoka et al. (Yamaoka et al., 1981) and represent the concentration required to inhibit cell viability by 50 %.

Fig. 3. *In vitro* antitumor activity of 4-HPR and 4-HPR encapsulated in polymeric micelles against B16BL6 cells. (A) Time and concentration dependence of *in vitro* antitumor activity of 4-HPR. Cell viability was measured by MTT method at 8 h (open circle), 16 h (open triangle), 24 h (filled circle), 48 h (filled triangle), and 72 h (filled square) after treatment. (B) *In vitro* antitumor activity of 4-HPR (open circle), empty polymeric micelles (shade triangle), and 4-HPR encapsulated in polymeric micelles (filled square) at 48 h after treatment. Each value represents the mean ± S.D. (n = 3–4).

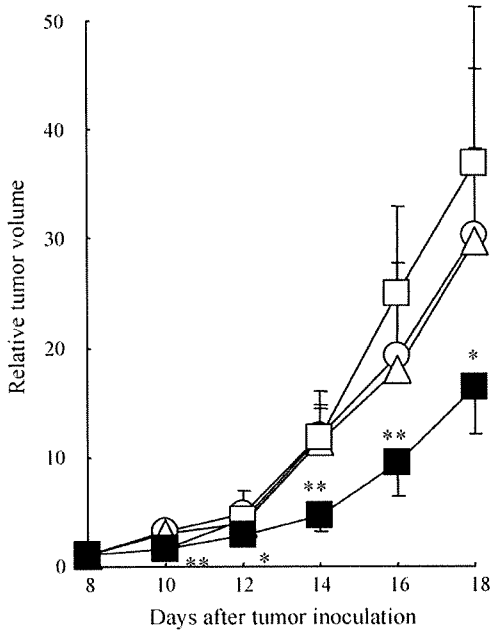

Fig. 5. Relative tumor volume of B16BL6-bearing mice after intravenous injection of PBS (open circle), empty polymeric micelles (open triangle), 4-HPR encapsulated in O/W emulsions (open square), and 4-HPR encapsulated in polymeric micelles (filled square). 4-HPR encapsulated in O/W emulsions and 4-HPR encapsulated in polymeric micelles were intravenously injected into mice at a dose of 75 mg/kg as 4-HPR on 8, 10, 12 days after tumor inoculation. The dose of empty polymeric micelles was 375 mg/kg as polymer, which was equivalent dose to 4-HPR encapsulated in polymeric micelles. Each value represents the mean ± S.D. (n = 6–12). Statistically significant differences compared with PBS-treated groups (**P < 0.01; *P < 0.05).

three times) after tumor inoculation. Only 4-HPR encapsulated in polymeric micelles significantly delayed tumor growth in B16BL6-bearing mice as compared with PBS (Fig. 5), while did not cause any significant weight loss (data not shown). On 18 days after tumor inoculation, approximately 55% of tumor growth inhibition was observed in mice treated with 4-HPR encapsulated in polymeric micelles. On the other hand, empty polymeric micelles and 4-HPR encapsulated in O/W emulsions did not have any effect on tumor growth (Fig. 5).

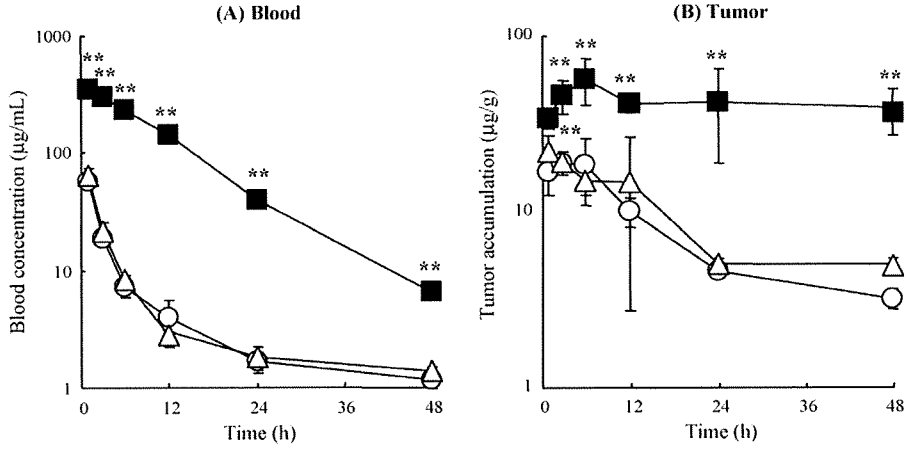

Fig. 4. Blood concentration (A) and tumor accumulation (B) of 4-HPR following intravenous injection of 4-HPR encapsulated in O/W emulsions (open circle), 4-HPR encapsulated in PEGylated O/W emulsions (open triangle), and 4-HPR encapsulated in polymeric micelles (filled square), into B16BL6-bearing mice. Each formulation was intravenously injected at 75 mg/kg dose of 4-HPR on 14 days after tumor inoculation. At indicated time point, blood and tumor were collected and amount of 4-HPR was measured by HPLC. Each value represents the mean ± S.D. (n = 3–6). Statistically significant differences compared with 4-HPR encapsulated in O/W emulsions (**P < 0.01).

Table 1
Pharmacokinetic parameters for blood and tumor concentration of 4-HPR after intravenous injection of 4-HPR encapsulated in polymeric micelles, 4-HPR encapsulated in O/W emulsions, and 4-HPR encapsulated in PEGylated O/W emulsions into B16BL6-bearing mice.

Formulation	$t_{1/2}$ (h)	$AUC_{0-\infty}$ (μg h/mL)	CL_{tot} (mL/h kg)	V_{dss} (mL/kg)	MRT (h)
Blood[a]					
O/W emulsions	1.73	197	382	843	2.21
PEGylated O/W emulsions	1.73	225	333	737	2.21
Polymeric micelles	8.68	4717	15.9	199	12.5

Formulation	C_{max} (μg/g)	T_{max} (h)	$t_{1/2}$ (h)	$AUC_{0-\infty}$ (μg h/g)	CL_{tot} (g/h kg)	V_{dss} (g/kg)	MRT (h)
Tumor							
O/W emulsions	18.7	3	17.7	430	175	4242	14.3
PEGylated O/W emulsions	21.7	1	20.1	509	147	4038	27.4
Polymeric micelles	56.6	6	99.8	7264	10.3	1505	146

$t_{1/2}$ = half-life; AUC = area under the curve; CL_{tot} = total body clearance; V_{dss} = volume of distribution at steady state; MRT = mean residence time; C_{max} = maximum concentration; T_{max} = time of maximum concentration; parameters were calculated from the mean value of three to six mice by moment analysis developed by Yamaoka et al. (1978).
[a] Parameters in blood were calculated for the initial phase of the experiment until 6 h after intravenous injection.

4. Discussion

Nano-particulate formulation is very attractive for intravenous injection of lipophilic drugs including 4-HPR. Previously, we have developed poly(ethylene glycol)–poly(aspartate) block copolymer micelles modified with benzyl groups and demonstrated their properties of stable encapsulation and enhanced blood circulation time of 4-HPR in mice (Okuda et al., 2008). In this study, we further investigated its disposition characteristics and pharmacological effects of 4-HPR encapsulated in polymeric micelles in tumor-bearing mice. We demonstrated here for the first time that *in vivo* antitumor effect was achieved by intravenous injection of 4-HPR encapsulated in polymeric micelles.

Spaces in the blood endothelium formed by solid tumors were reported to range between 300 and 4700 nm (Yuan et al., 1995; Hashizume et al., 2000). As shown in Fig. 2, the mean particle size of prepared polymeric micelles was approximately 173 nm. Furthermore, their mean particle size did not change for more than 1 month storage, even at room temperature (data not shown). These results suggested that they might be small enough to exert long circulating potential and pass through the endothelium of solid tumors.

As shown in Fig. 3(A), exposure to 4-HPR for more than 24 h was needed to exert high antitumor activity of 4-HPR against B16BL6 cells *in vitro*. This observation of *in vitro* antitumor characteristics of 4-HPR corresponds with a previous report (Wu et al., 2005) and in the other cancer cells (Holmes et al., 2003). Since EPR effects are known to enhance and prolong tumor distribution based on the characteristic vascular structure around tumor tissues, such passive targeting of 4-HPR to tumor tissues by EPR effects is expected to be an effective strategy for exerting *in vivo* pharmacological actions. After intravenous injection of 4-HPR encapsulated in polymeric micelles, the blood concentration of 4-HPR was extended (Fig. 4(A)). Investigating whether polymeric micelles can improve *in vivo* antitumor efficacy of 4-HPR, and the therapeutic efficacy of 4-HPR encapsulated in polymeric micelles was evaluated in B16BL6-bearing mice. As shown in Fig. 4(B), the tumor concentration of 4-HPR by 4-HPR encapsulated in polymeric micelles was from 33.9 to 56.6 μg/g of 4 HPR for 48 h and could significantly inhibit tumor growth (Fig. 5). The *in vivo* antitumor efficacy might be supported by the fact that *in vitro* IC_{50} value of 4-HPR against B16BL6 cells at more than 24 h was approximately 0.60 μg/mL. *In vitro* antitumor activity of 4-HPR encapsulated in polymeric micelles was much lower than that of 4-HPR in free form (Fig. 4(B)), but intravenously injected 4-HPR encapsulated in polymeric micelles showed the enhanced antitumor efficacy *in vivo* (Fig. 5). It might be partly explained that stably encapsulated 4-HPR was much slowly released in medium but was a little enhanced releasing by interaction with various biocomponents such as serum albumin and blood cells *in vivo*. With regard to the toxicity of 4-HPR encapsulated in polymeric micelles, no significant loss of body weight was observed in treated mice, suggesting little severe toxicity (data not shown). These results lead us to believe that enhanced *in vivo* antitumor efficacy of 4-HPR could be achieved by polymeric micelles without severe side-effects.

Lipid particles are known as conventional drug carriers, and have been already used clinically (Tamilvanan, 2004; Torchilin, 2005). In particular, O/W emulsions or PEGylated O/W emulsions can dissolve highly lipophilic drugs in the inner oil phase; however, few reports are available to compare the disposition of lipophilic drugs by encapsulation into polymeric micelles with that in these emulsions. After intravenous injection of 4-HPR encapsulated in O/W emulsions and PEGylated O/W emulsions, 4-HPR were rapidly eliminated from the blood and tumor (Fig. 4). Similarly, *in vivo* antitumor efficacy by 4-HPR encapsulated in O/W emulsion was not observed (Fig. 5). In our previous study, we systematically investigated the *in vivo* disposition of drugs with diverse lipophilicity, and concluded that the required lipophilicity of drugs for stable encapsulation into O/W emulsions was found to be 10^9 based on the partition coefficient between n-octanol and water (PC_{oct}) values (Takino et al., 1994). PC_{oct} of 4-HPR is $10^{8.03}$ (Kokate et al., 2007); therefore, 4-HPR might be rapidly released from O/W emulsions and PEGylated O/W emulsions to the blood stream by the intravenous injection.

Many factors can contribute to tumorigenesis, including inherited and acquired genetic changes, chromosomal rearrangements, epigenetic phenomena and chemical carcinogenesis. Retinoids can interfere with these events on several levels, their principal known actions being the induction of differentiation and apoptosis of tumor cells, and inhibition of tumor promotion in chemically induced cancers (Means and Gudas, 1995; Kagechika and Shudo, 2005). To date, many retinoids are candidates for the treatment of cancers (Altucci and Gronemeyer, 2001; Clarke et al., 2004); however, it is difficult to achieve therapeutic effect under *in vivo* conditions because their highly lipophilic nature and teratogenicity (Collins and Mao, 1999; Soprano and Soprano, 1995). In order to overcome these problems, we developed poly(ethylene glycol)–poly(benzyl aspartate) block copolymer micelles for 4-HPR delivery. In polymeric micelle delivery, drug encapsulation characteristics can be controlled by modification of the hydrophobic segments of block copolymers (Yokoyama et al., 2004; Watanabe et al., 2006; Okuda et al., 2008). Taking these into consideration, polymeric micelles would be effective carriers for various retinoids for cancer chemotherapy in the future.

In conclusion, we have examined the biodistribution characteristics of 4-HPR encapsulated in poly(ethylene glycol)–poly(benzyl

aspartate) block copolymer micelles after intravenous injection in tumor-bearing mice. We have demonstrated that 4-HPR encapsulated in polymeric micelles sustained blood retention of 4-HPR, passive accumulation at tumor sites, and led to superior therapeutic benefits of 4-HPR against solid tumor in tumor-bearing mice.

Acknowledgements

This work was supported in part by Grants-in-Aid for Scientific Research from the Ministry of Education, Culture, Sports, Science, and Technology of Japan, and by Health and Labour Sciences Research Grants for Research on Advanced Medical Technology from the Ministry of Health, Labour and Welfare of Japan. T. Satoh, Y. Oka, and M. Yokoyama acknowledge support by the Program for Promoting the Establishment of Strategic Research Centers, Special Coordination Funds for Promoting Science and Technology, The Ministry of Education, Culture, Sports, Science, and Technology, Japan.

References

Altucci, L., Gronemeyer, H., 2001. The promise of retinoids to fight against cancer. Nat. Rev. Cancer 1, 181–193.
Chansri, N., Kawakami, S., Yamashita, F., Hashida, M., 2006. Inhibition of liver metastasis by all-trans retinoic acid incorporated into O/W emulsions in mice. Int. J. Pharm. 321, 42–49.
Chansri, N., Kawakami, S., Yokoyama, M., Yamamoto, T., Charoensit, P., Hashida, M., 2008. Anti-tumor effect of all-trans retinoic acid loaded polymeric micelles in solid tumor bearing mice. Pharm. Res. 25, 428–434.
Clarke, N., Germain, P., Altucci, L., Gronemeyer, H., 2004. Retinoids: potential in cancer prevention and therapy. Expert Rev. Mol. Med. 6, 1–23.
Collins, M.D., Mao, G.E., 1999. Teratology of retinoids. Annu. Rev. Pharmacol. Toxicol. 39, 399–430.
Corazzari, M., Lovat, P.E., Oliverio, S., Di Sano, F., Donnorso, R.P., Redfern, C.P., Piacentini, M., 2005. Fenretinide: a p53-independent way to kill cancer cells. Biochem. Biophys. Res. Commun. 331, 810–815.
Hail Jr., N., Kim, H.J., Lotan, R., 2006. Mechanisms of fenretinide-induced apoptosis. Apoptosis 11, 1677–1694.
Hashizume, H., Baluk, P., Morikawa, S., McLean, J.W., Thurston, G., Roberge, S., Jain, R.K., McDonald, D.M., 2000. Openings between defective endothelial cells explain tumor vessel leakiness. Am. J. Pathol. 156, 1363–1380.
Holmes, W.F., Soprano, D.R., Soprano, K.J., 2003. Comparison of the mechanism of induction of apoptosis in ovarian carcinoma cells by the conformationally restricted synthetic retinoids CD437 and 4-HPR. J. Cell. Biochem. 89, 262–278.
Hultin, T.A., May, C.M., Moon, R.C., 1986. N-(4-hydroxyphenyl)-all-trans-retinamide pharmacokinetics in female rats and mice. Drug Metab. Dispos. 14, 714–717.
Kagechika, H., Shudo, K., 2005. Synthetic retinoids: recent developments concerning structure and clinical utility. J. Med. Chem. 48, 5875–5883.
Kataoka, K., Harada, A., Nagasaki, Y., 2001. Block copolymer micelles for drug delivery: design, characterization and biological significance. Adv. Drug Deliv. Rev. 47, 113–131.
Kawakami, S., Opanasopit, P., Yokoyama, M., Chansri, N., Yamamoto, T., Okano, T., Yamashita, F., Hashida, M., 2005. Biodistribution characteristics of all-trans retinoic acid incorporated in liposomes and polymeric micelles following intravenous administration. J. Pharm. Sci. 94, 2606–2615.
Kawakami, S., Suzuki, S., Yamashita, F., Hashida, M., 2006. Induction of apoptosis in A549 human lung cancer cells by all-trans retinoic acid incorporated in DOTAP/cholesterol liposomes. J. Control. Release 110, 514–521.
Kokate, A., Li, X., Jasti, B., 2007. Transport of a novel anti-cancer agent, fenretinide across Caco-2 monolayers. Invest. New Drugs 25, 197–203.
Kwon, G.S., 2003. Polymeric micelles for delivery of poorly water-soluble compounds. Crit. Rev. Ther. Drug Carrier Syst. 20, 357–403.
Maeda, H., 2001. The enhanced permeability and retention (EPR) effect in tumor vasculature: the key role of tumor-selective macromolecular drug targeting. Adv. Enzyme Regul. 41, 189–207.
Means, A.L., Gudas, L.J., 1995. The roles of retinoids in vertebrate development. Annu. Rev. Biochem. 64, 201–233.
Miller Jr., W.H., 1998. The emerging role of retinoids and retinoic acid metabolism blocking agents in the treatment of cancer. Cancer 83, 1471–1482.
Moon, R.C., Thompson, H.J., Becci, P.J., Grubbs, C.J., Gander, R.J., Newton, D.L., Smith, J.M., Phillips, S.L., Henderson, W.R., Mullen, L.T., Brown, C.C., Sporn, M.B., 1979. N-(4-hydroxyphenyl)retinamide, a new retinoid for prevention of breast cancer in the rat. Cancer Res. 39, 1339–1346.
Okuda, T., Kawakami, S., Yokoyama, M., Yamamoto, T., Yamashita, F., Hashida, M., 2008. Block copolymer design for stable encapsulation of N-(4-hydroxyphenyl)retinamide into polymeric micelles in mice. Int. J. Pharm. 357, 318–322.
Opanasopit, P., Yokoyama, M., Watanabe, M., Kawano, K., Maitani, Y., Okano, T., 2004. Block copolymer design for camptothecin incorporation into polymeric micelles for passive tumor targeting. Pharm. Res. 21, 2001–2008.
Soprano, D.R., Soprano, K.J., 1995. Retinoids as teratogens. Annu. Rev. Nutr. 15, 111–132.
Swanson, B.N., Zaharevitz, D.W., Sporn, M.B., 1980. Pharmacokinetics of N-(4-hydroxyphenyl)-all-trans-retinamide in rats. Drug Metab. Dispos. 8, 168–172.
Takino, T., Konishi, K., Takakura, Y., Hashida, M., 1994. Long circulating emulsion carrier systems for highly lipophilic drugs. Biol. Pharm. Bull. 17, 121–125.
Tamilvanan, S., 2004. Oil-in-water lipid emulsions: implications for parenteral and ocular delivering systems. Prog. Lipid Res. 43, 489–533.
Torchilin, V.P., 2004. Targeted polymeric micelles for delivery of poorly soluble drugs. Cell. Mol. Life Sci. 61, 2549–2559.
Torchilin, V.P., 2005. Recent advances with liposomes as pharmaceutical carriers. Nat. Rev. Drug Discov. 4, 145–160.
Villablanca, J.G., Krailo, M.D., Ames, M.M., Reid, J.M., Reaman, G.H., Reynolds, C.P., 2006. Phase I trial of oral fenretinide in children with high-risk solid tumors: a report from the Children's Oncology Group (CCG 09709). J. Clin. Oncol. 24, 3423–3430.
Watanabe, M., Kawano, K., Yokoyama, M., Opanasopit, P., Okano, T., Maitani, Y., 2006. Preparation of camptothecin-loaded polymeric micelles and evaluation of their incorporation and circulation stability. Int. J. Pharm. 308, 183–189.
Wu, X.Z., Zhang, L., Shi, B.Z., Hu, P., 2005. Inhibitory effects of N-(4-hydrophenyl) retinamide on liver cancer and malignant melanoma cells. World J. Gastroenterol. 11, 5763–5769.
Yamaoka, K., Nakagawa, T., Uno, T., 1978. Statistical moments in pharmacokinetics. J. Pharmacokinet. Biopharm. 6, 547–558.
Yamaoka, K., Tanigawara, Y., Nakagawa, T., Uno, T., 1981. A pharmacokinetic analysis program (multi) for microcomputer. J. Pharmacobiodyn. 4, 879–885.
Yokoyama, M., Opanasopit, P., Okano, T., Kawano, K., Maitani, Y., 2004. Polymer design and incorporation methods for polymeric micelle carrier system containing water-insoluble anti-cancer agent camptothecin. J. Drug Target 12, 373–384.
Yuan, F., Dellian, M., Fukumura, D., Leunig, M., Berk, D.A., Torchilin, V.P., Jain, R.K., 1995. Vascular permeability in a human tumor xenograft: molecular size dependence and cutoff size. Cancer Res. 55, 3752–3756.

In Vivo and *In Vitro* Evaluation of Gelation and Hemostatic Properties of a Novel Tissue-Adhesive Hydrogel Containing a Cross-Linkable Polymeric Micelle

Yoshihiko Murakami,[1] Masayuki Yokoyama,[2] Hiroshi Nishida,[3] Yasuko Tomizawa,[3] Hiromi Kurosawa[3]

[1] Department of Organic and Polymer Materials Chemistry, Tokyo University of Agriculture and Technology, Tokyo, Japan

[2] Yokoyama Nano-Medical Polymers Project, Kanagawa Academy of Science and Technology (KAST), Takatsu, Kawasaki, Kanagawa 213-0012, Japan

[3] Department of Cardiovascular Surgery, The Heart Institute of Japan, Tokyo Women's Medical University, Shinjuku, Tokyo 162-8666, Japan

Received 3 July 2008; revised 16 January 2009; accepted 6 February 2009
Published online 22 April 2009 in Wiley InterScience (www.interscience.wiley.com). DOI: 10.1002/jbm.b.31378

Abstract: There is a clinical requirement for a local hemostat that arrests bleeding from both suture holes and cross-sectional surfaces of parenchymatous organs. A novel tissue-adhesive hydrogel was prepared that contains a cross-linkable polymeric micelle consisting of poly(ethylene glycol)-poly(DL-lactide) block polymers, and, by means of a rheometer, the factors that affect the hydrogel's gelation properties was clarified. The storage modulus and the gelation time greatly depended on both the pH and the concentrations of both the polymeric micelle and polyallylamine solutions. Furthermore, the hemostatic potential of the hydrogel in a mouse hemostasis model was evaluated under optimal conditions as determined by the rheometer. The average amount of bleeding from the mouse liver was 172.9 mg (S.D. 69.7 mg, $N = 7$) in the control experiments, whereas it was 20.1 mg (s.d. 13.2, $N = 7$) when the hydrogel was applied to the wound ($p = 0.002$). The result demonstrated that the novel synthetic hydrogel possessed a significant hemostatic potential as a local hemostat. © 2009 Wiley Periodicals, Inc. J Biomed Mater Res Part B: Appl Biomater 91B: 102–108, 2009

Keywords: tissue-adhesive hydrogel; hemostat; polymeric micelle; block polymer; tissue sealant

INTRODUCTION

There is a clinical requirement for a local hemostat that arrests bleeding from both suture holes and cross-sectional surfaces of parenchymatous organs.[1] The use of a local hemostat is a requisite wherein the use of cautery, ligature, or other conventional hemostatic methods is impractical. Currently, several tissue-adhesive local hemostatic formulations have been developed for surgical applications. The local hemostats include fibrin-based glues,[2,3] collagen-based glues (collagen sheets with fibrin glues,[4] fibrillar collagen,[5] and collagen containing a citric acid derivative[6]), gelatin with resorcin and formalin (GRF glue™),[7] albumin with glutaraldehyde (Bioglue™),[8] and synthetic polymer-based glues (cyanoacrylate[9] and synthetic polymers[10–13]). However, none of these hemostats functions in a completely satisfactory manner. The potential risk of infectious contamination is a major drawback for fibrin-, collagen-, and gelatin-based glues.[3,14–17] The glues that contain low-molecular-weight aldehydes (e.g., formaldehyde and glutaraldehyde) as cross-linkers are extremely cytotoxic because they can penetrate into tissues owing to their highly diffusive nature.[18,19] Synthetic polymer-based glues have been actively developed because they do not pose any risk of infectious contaminations. Essential properties for the synthetic glues are absorbability, biodegradability, nontoxicity, and reactivity in physiological conditions. The molecular design of polymers can easily control these properties. However, complicated preparation procedures[10–13] required for some of the synthetic glues make their application difficult and nearly impossible in case of hemorrhage.

Recently, we reported that a novel hydrogel containing a cross-linkable polymeric micelle that formed from poly (ethylene glycol)-poly(DL-lactide) (PEG-PLA) block polymers had tissue-adhesive properties.[20] A polymeric micelle

Correspondence to: Y. Murakami (e-mail: muray@cc.tuat.ac.jp) or M. Yokoyama (e-mail: yp-yokoyama2093ryo@newkast.or.jp)
Contract grant sponsors: Ministry of Education, Culture, Sports, Science and Technology of Japan; New Energy and Industrial Technology Development Organization (NEDO) of Japan

is a macromolecular spherical particle (molecular weight: ca. several millions Da). We could easily transform the micelle into highly reactive another component by using aldehyde-terminated block polymers. The expectation was that the reactive polymeric micelles would have low-tissue permeability owing to the exceptionally high-molecular weights (ca. several millions) of the polymeric micelles. Therefore, the hydrogels forming form the reactive polymeric micelles are expected show very low risk of tissue damage, which caused through tissue permeation of the unreacted polymeric micelles. Furthermore, the hydrogel can release drug in a controlled manner, since the micelle inner core has been known to work as a drug container. The resulting hydrogel adhered to a tissue because of the Schiff base formation between the aldehyde groups on the polymeric micelle surface and the amino groups that are present on the tissue surface (e.g., primary amino groups of cell adhesion molecules and lipids). Measurements by means of a coagulometer showed that the hydrogel was rapidly formed when the polymeric micelle and polyallylamine solutions were mixed. However, it was difficult to evaluate factors affecting the hydrogel's gelation properties by means of a coagulometer because a coagulometer can facilitate monitoring of the gelation process only in the process's early stage (within a few seconds). Furthermore, it was not demonstrated whether the novel tissue-adhesive hydrogel could be used as a local hemostat in the previous paper.

In this study, the factors affecting the gelation properties of the novel tissue-adhesive hydrogel was evaluated by using a rheometer instead of coagulometer that was used in the previous paper. A rheometer can quantitatively determine viscoelastic properties of materials during the long-time operation (not only within a few seconds). The viscoelastic properties are important to the design of effective local hemostats. In addition, this is the first report which shows that the easily prepared synthetic hydrogel possessed a significant hemostatic potential as a local hemostat by using mice hemostasis model.

MATERIALS AND METHODS

Materials

Ethylene oxide (Sumitomo Seika Chemicals Co., Osaka, Japan) was purified by distilling it with CaH_2. DL-Lactide (Tokyo Chemical Industry Co., Tokyo, Japan) was recrystallized twice from ethyl acetate. To purify 3,3-diethoxypropanol, we distilled it with sodium under reduced pressure. Potassium naphthalene was obtained by mixing potassium and naphthalene in anhydrous tetrahydrofuran for 18 h. Polyallylamine (PAA) hydrochloride with an average molecular weight of 60,000 was kindly provided by Nitto Boseki Co., (Japan). All the other reagents were of analytical grade and were used without further purification.

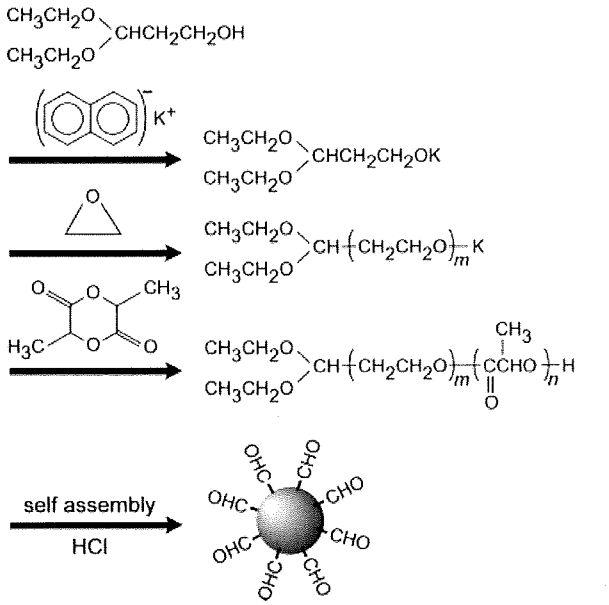

Figure 1. Scheme for the preparation of an aldehyde-terminated polymeric micelle.

Preparation of an Aldehyde-Terminated Polymeric Micelle Forming From PEG-PLA Block Polymers

An aldehyde-terminated polymeric micelle consisting of PEG-PLA block polymers was prepared according to the previously reported method[21] with slight modifications. Figure 1 shows the scheme for the micelle preparation. First, acetal-terminated PEG-PLA was obtained by employing anionic ring-opening polymerization of both ethylene oxide and DL-lactide in anhydrous tetrahydrofuran. 3,3-Diethoxypropanol (1 mmol) and potassium naphthalene (1 mmol) were mixed in tetrahydrofuran for 2 h. The purified ethylene oxide (105 mmol) was added to the obtained potassium 3,3-diethoxypropoxide solution (50 mL). After stirring for 48 h, 31 mmol of the purified DL-lactide was added to the solution. The resulting polymer, acetal-terminated PEG-PLA, was precipitated into ice-cold 2-propanol, stored in a freezer for 12 h, centrifuged at 12,000 rpm for 30 min, and lyophilized in benzene. The number-average molecular weight of the acetal-terminated block polymer was 7500 (PEG and PLA units were 4640 and 2860, which were determined on the basis of a gel permeation chromatography and of ^{1}H NMR, respectively). ^{1}H NMR also showed that the acetal group was introduced to 100% of the terminus of the polymer. We dissolved the acetal-terminated PEG-PLA in *N,N*-dimethylacetamide and then performed dialysis against water by using a Spectra/Por7 dialysis membrane (molecular weight cut-off: 1 kDa; Spectrum, Houston, TX) for 24 h. HCl was added to the polymeric micelle solution to adjust pH to 2. The solution was mixed for 2 h to convert the acetal group into an aldehyde group on the surface of the micelle. To stop the reaction, the pH of the solution was adjusted to 5 by adding an aqueous